Summer 2014

Design and Analysis of Circularly Polarized Electrically Small Antennas

Jesse R. Ludwig

DESIGN AND ANALYSIS OF CIRCULARLY POLARIZED ELECTRICALLY SMALL ANTENNAS

by

JESSE R. LUDWIG

(Under the Direction of Professor Sungkyun Lim)

ABSTRACT

A growing need for efficient wireless communication is prevalent in the world in which we live. From cell phones to television to GPS applications, wireless communications are vital in consumer electronics and military applications. In these applications, a miniaturized antenna is sometimes necessary for reducing overall size of the communication system. For many satellite based communication applications, circular polarization in antennas is needed for efficient communication. In this thesis, the miniaturization technique known as T-top loading is utilized on two novel antenna designs. One design is an electrically small, circularly polarized planar cross dipole and the other design is a compact circularly polarized log-periodic dipole array. Both antennas are designed in simulation software with the intent for prototype fabrication for measurement verification of simulation results.

INDEX WORDS: Antenna, antenna optimization, electrically small antenna, circular polarization, genetic alogrithm, LPDA, miniaturization, planar antenna, top-loading.

DESIGN AND ANALYSIS OF CIRCULARLY POLARIZED ELECTRICALLY SMALL ANTENNAS

by

JESSE R. LUDWIG

B.S.E.E.T., Georgia Southern University, GA., USA, 2012

A Thesis Submitted to the Graduate Faculty of Georgia Southern University in Partial

Fulfillment

of the Requirements for the Degree

MASTER OF SCIENCE

STATESBORO, GEORGIA

2013

DESIGN AND ANALYSIS OF CIRCULARLY POLARIZED ELECTRICALLY SMALL ANTENNAS

by

JESSE R. LUDWIG

Major Professor:	Sungkyun Lim
Committee:	Mohammad Ahad
	Fernando Rios-Gutierrez

Electronic Version Approved:
July 2014

ACKNOWLEDGMENTS

I would first like to thank my family first for their continuous support and encouragement. I'm thankful for the research opportunity I've received from Professor Sungkyun Lim, for all the help with my research from everyone working in the antennas laboratory at Georgia Southern University, and for all the faculty's help and teachings in the engineering department.

ABBREVIATION

CP	Circular Polarization
LPDA	Log-Periodic Dipole Array
GA	Genetic Algorithm
PCD	Planar Cross Dipole

TABLE OF CONTENTS

LIST OF FIGURES

CHAPTER 1

INTRODUCTION

1.1 Role and Characteristics of Antennas in Communication Systems

In the past decade, wireless communication via electromagnetic waves has been on the rise in popularity, giving birth to many industries involved in implementation and research of producing more effective wireless communication systems. Wireless communication in the electromagnetic spectrum offers many advantages compared to audible and visual communication. These advantages include a longer range of propagation (audible) and independence from line-of-sight (visual). Just as noise affects a person's ability to hear one particular person in a crowd of talking people, communication systems can be affected by electromagnetic noise. The radiator component that sends and receives information in a communication system, the antenna, can be seen as a band-pass filter that allows only electromagnetic waves within a certain frequency range be accepted by the communication system, resulting in the rejection of noise outside of the frequency range. Therefore, the antenna's characteristics are important to the communication system, and the antenna can be manipulated to vary in size and shape to fit the space requirements of the communication system.

Another important aspect to consider of the antenna is polarization. Three types of polarization exist: linear, circular, and elliptical. An antenna that is linearly polarized is direction-sensitive and is commonly used in horizontal polarization or vertical polarization. In the case of a simple antenna such as a dipole, horizontal polarization would be when the antenna is oriented parallel to the ground, and vertical polarization

would be when the antenna is oriented perpendicular to the ground. When two dipoles are oriented in differing polarizations (one horizontal and one vertical), the polarization mismatch results in very poor communication performance. Circular polarization occurs when a time-harmonic wave, at a given point in space, has an electric field vector that traces a circle as a function of time. Basically, the field vector must have two orthogonal linear components of the same magnitude that have a time-phase difference of odd multiples of 90° (Balanis 2005). Elliptical polarization consists of any polarization that is neither linear nor circular polarization. The popular method of describing the polarization of an antenna is by axial ratio, which is the ratio of the magnitude of the major and minor axes defined by the electric field vector. Axial ratio is commonly measured in decibels, and an axial ratio lower than 3 dB is considered circularly polarized. The advantages of circular polarization include independence from polarization of the transmitter/receiver antenna, improved propagation through earth's ionosphere, and reduction of multi-path interference. However, circular polarization must be implemented by some kind of special feeding network or the antenna must be circularly polarized, which usually results in a larger antenna size.

The earliest experiments of antennas occurred in the late 1800s, involving Joseph Henry's experiments with circuits and needles, and later a vertical wire on the roof of his house that was used to detect lightning flashes. Later, in 1875, Thomas Edison observed the radiation of a telegraph key closure, and patented the communication system in 1885. The communication system patented by Edison consisted of vertical top-loaded antennas (Stutzman 1998). Although unknown at the time, top-loading on antennas would prove to be an effective method of antenna miniaturization. On a simple wire antenna such as a

monopole, top-loading involves adding a wire to the end of the antenna such that the antenna and wire form a "T" shape connection. The currents in the wire on either side of the monopole cancel each other out, making the radiation from this segment far from the antenna negligible. The benefit of this added segment is added capacitance to the top of the antenna, which results in increased currents at the top of the main radiator (monopole). Ultimately, the efficiency of the antenna is improved because of increased radiation resistance, which drops when the antenna size is reduced. With methods of miniaturization such as top-loading, antennas can be made smaller while still operating efficiently in a communication system.

1.2 Electrically Small Antennas

With the widespread popularity of wireless technologies and the desire for smaller consumer electronics, the research and development of new antenna designs has been an area of much research. The demand for smaller antennas for use in communication systems within a limited space has increased for applications such as cell phones, blue tooth devices, GPS navigation devices, gaming systems, automobiles and aircrafts, and many more. However, with antenna miniaturization to meet the growing demand for smaller spaces, there is a trade-off which is in bandwidth and efficiency as related to the size of the antenna.

The size of an antenna is commonly represented in the form of its electrical length, which is the physical length of the antenna in relation to its operating frequency. In this way, a fair comparison can be made between physical antenna size and its operating frequency. For example, a half-wavelength dipole can be 10 m long, or 10 cm

long. The operating frequency of both dipoles is different, but the electrical length would be calculated to be the exact same. This comparison demonstrates that the antenna design's intrinsic characteristics affect the electrical size of the antenna rather than its operating frequency. An alternative way to represent an antenna's electrical length is by the formula:

$$kr = \frac{2\pi}{\lambda} \times r\ , \tag{1}$$

where k is defined as the wave number and r is the radius of the smallest sphere that encloses the entire antenna (Wheeler 1947). An example of the smallest sphere enclosing an antenna can be seen in Figure 1.1, where a half-wavelength dipole is shown. An antenna with a $kr < 1$ is considered electrically small.

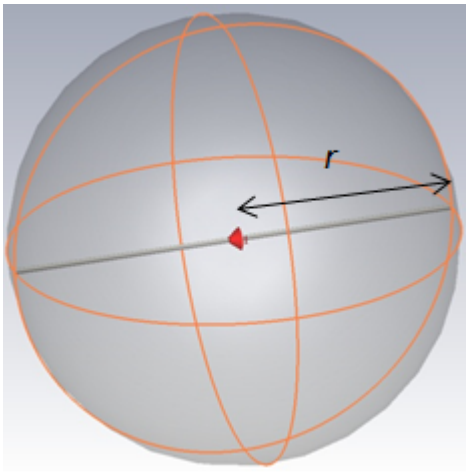

Figure 1.1. Sphere enclosing half-wavelength dipole.

With a reduction in an antenna's electrical size comes a trade-off in the form of bandwidth and efficiency. As an antenna's kr decreases, its radiation resistance drops and becomes less efficient. Various matching techniques such as top-loading are usually employed to overcome low radiation resistance. Figure 1.2 shows the theoretical maximum bandwidth of an antenna as related to its kr. For a reference, the location of a

dipole on the curve has been marked. A dipole has a 10 % fractional impedance bandwidth and a *kr* of about 1.6.

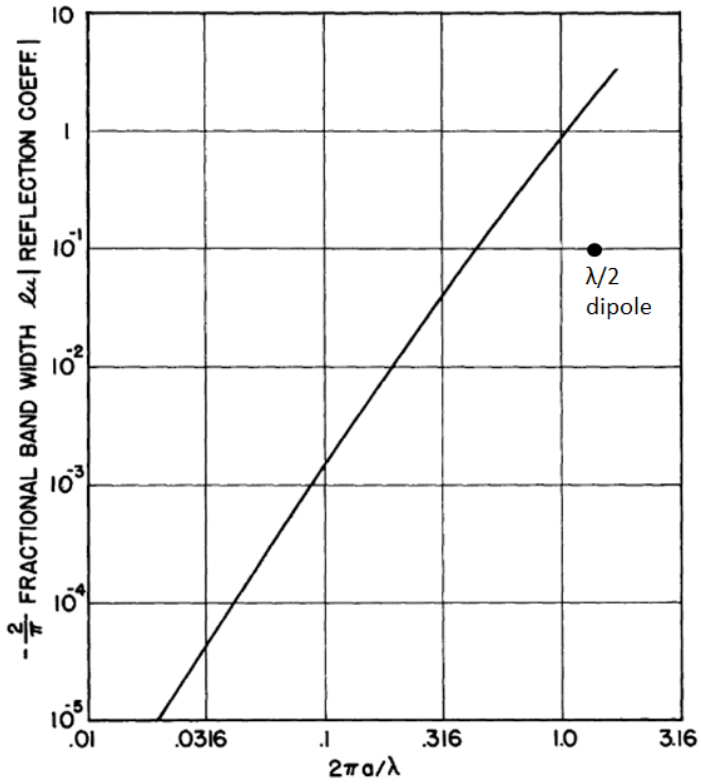

Figure 1.2. *kr* vs. theoretical maximum fractional impedance bandwidth (Chu 1948).

From this curve representing the theoretical maximum bandwidth possible, it is ideal for an antenna design to lie as close to the curve as possible, or on the curve if possible. For a specific application, an appropriate *kr* value must be selected to provide the required bandwidth. Generally, for single-frequency applications, reducing the *kr* of the antenna design as much as possible is preferred. An example of progression in the field of antenna miniaturization and efficiency can be seen in Figure 1.3, which shows a study consisting of 110 published antenna designs plotted against the *kr* vs. bandwidth theoretical maximum limit (Sievenpiper, et al. 2012). The study states that the design

above the limit does not actually exceed the limit (the discrepancy is due to a matching circuit). Several antennas come close to the limit, but more improvements are still to be made in antenna miniaturization.

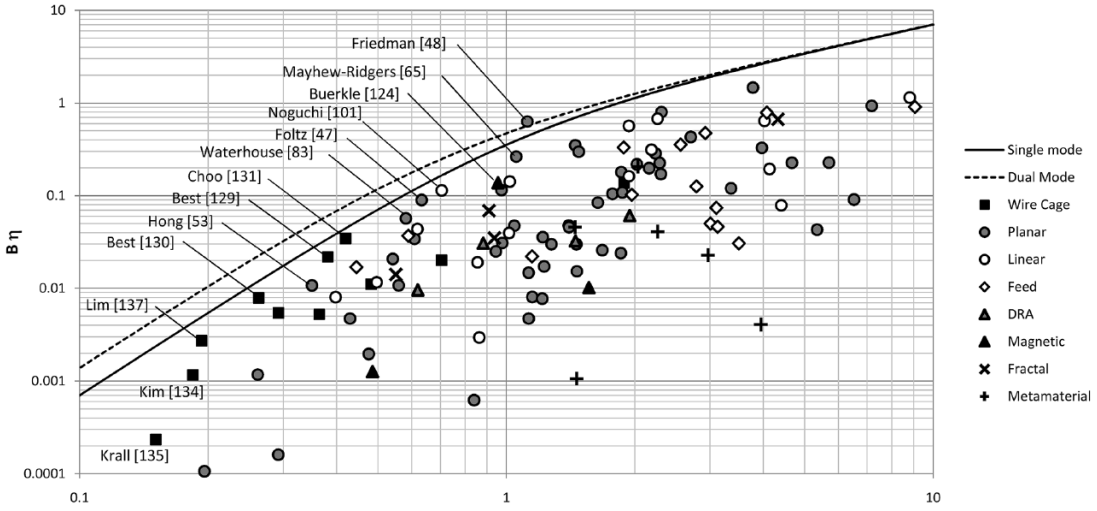

Figure 1.3. *kr* vs. theoretical maximum bandwidth of published antenna designs (Sievenpiper, et al. 2012).

1.3 Previous Research in Antenna Miniaturization Techniques

Many research publications have been presented in the past several decades in the field of antennas and miniaturization techniques. These publications are important in discovering trends in antenna design and understanding the latest technology in antenna miniaturization. Previously, various miniaturization techniques have been presented in published literature that are similar to novel antenna designs presented in this thesis. Section 1.3.1 presents past research in electrically small, circularly polarized planar antennas and section 1.3.2 presents past research in miniaturization techniques in log-period dipole arrays.

1.3.1 Electrically Small, Circularly Polarized Planar Antennas

Planar antennas or printed designs have become a popular choice for integration into mobile and portable communication systems due to their low-cost, low-weight, low-profile, and easily manufactured structures. Although planar antennas offer many advantages over traditional three-dimensional antenna designs, developing a planar antenna that is both electrically small and circularly polarized (CP) has been considered challenging to achieve. Previously, a truncated planar CP antenna for UHF RFID was presented (Suwalak and Phongcharoenpanich 2007). The antenna structure, shown in Figure 1.4, employed a substrate consisting of 3 layers with truncated corners, allowing CP to be generated with a single-point feed. The electrical size, *kr*, of the antenna is 2.13.

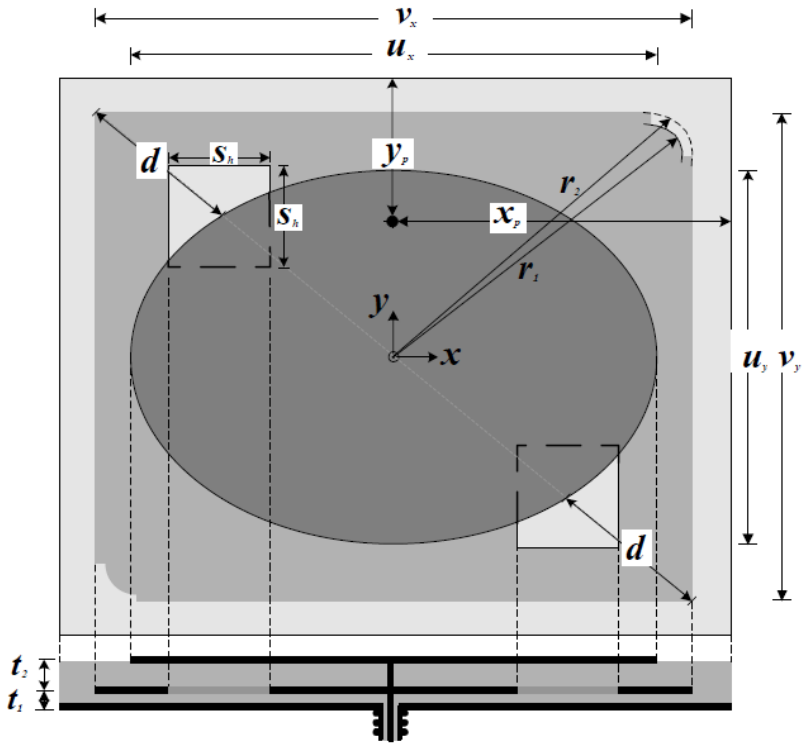

Figure 1.4. Single-feed, circularly polarized truncated planar antenna (Suwalak and Phongcharoenpanich 2007).

Another single-point feed CP planar antenna is presented in Figure 1.5 (Nalbandian and Lee 1998). The antenna consists of two radiating patches separated by a metal substrate. Small holes connecting the upper and lower patches allow CP to be generated by creating a 90 degree phase shift between radiation elements. The antenna has an electrical size, *kr*, of 1.59.

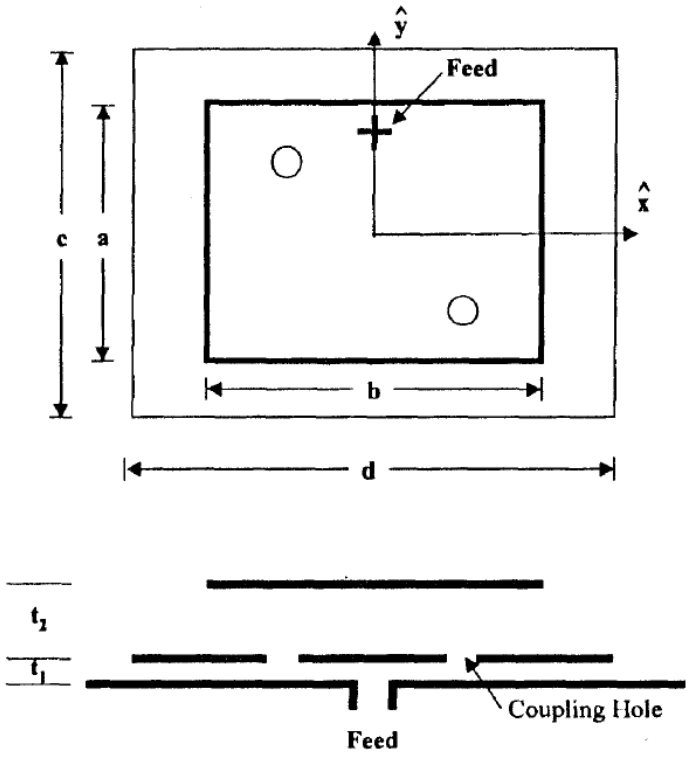

Figure 1.5. Single-feed, circularly polarized planar microstrip antenna (Nalbandian and Lee 1998).

Recently, a wideband, subwavelength resonator antenna is reported in a study (Bai, et al. 2013). The geometry of the antenna, in Figure 1.6, consisted of two coupled D-shaped rings fed with a monopole-like matching network. While the antenna is electrically small ($kr = 0.49$) at the lowest operating frequency, it does not generate CP.

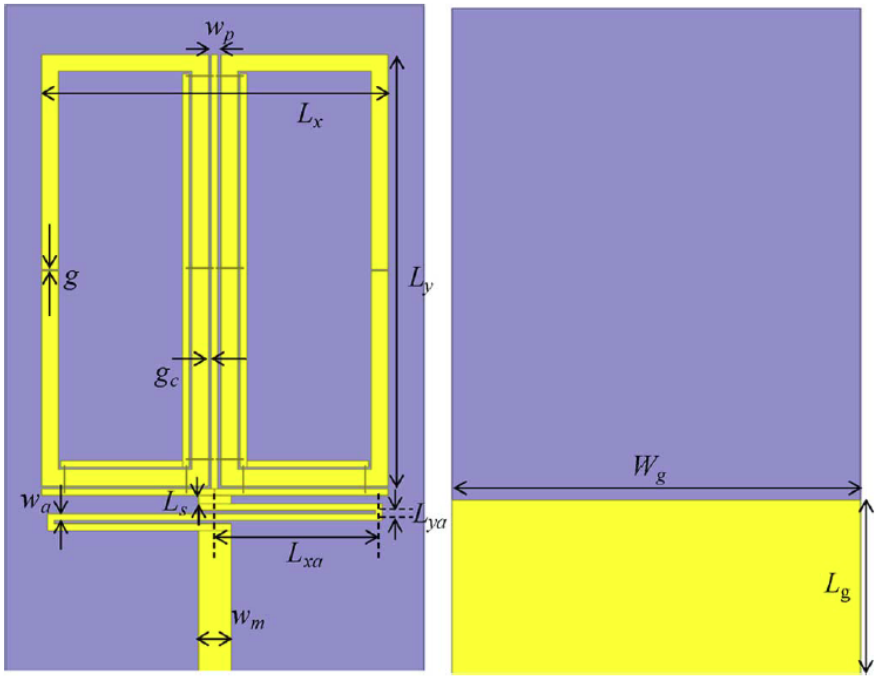

Figure 1.6. Planar, electrically small, coupled subwavelength resonator antenna design (Bai, et al. 2013).

1.3.2 Miniaturization Techniques Log-Periodic Dipole Arrays

Log-periodic dipole array (LPDA) antennas have been a popular choice in communications systems since their creation by Isbell (Isbell 1960), due to their wide impedance bandwidth coverage and high gain. One problem with LPDAs, however, is large antenna size since LPDAs are a combination of multiple elements of λ/2 dipoles with increasing space between dipole elements as the element lengths increase. With this reason, the LPDA is not feasible when space for the antenna is limited in a communication system. Thus, size reduction of LPDAs is desired to be more applicable in various communication environments with limited space or portable applications.

Previously, research studies for size reduction of LPDAs have been reported by miniaturizing the dipole elements of the LPDA. For example, the lengths of the four longest elements in the LPDA were reduced with the use of a ridged-waveguide

technique (Kuo 1970). The end result was a hybrid between a conventional LPDA and a size-reduced element LPDA, as shown in Figure 1.7. By reducing the length of the longest elements of the LPDA, the overall width of the LPDA could be reduced. The performance of the size-reduced LPDA resulted in a similar gain pattern as a conventional LPDA at the lowest operating frequency (frequency of the size-reduced elements), as shown in Figure 1.8. The author reports an overall width reduction of 40 % in the mixed element LPDA as compared to a conventional LPDA.

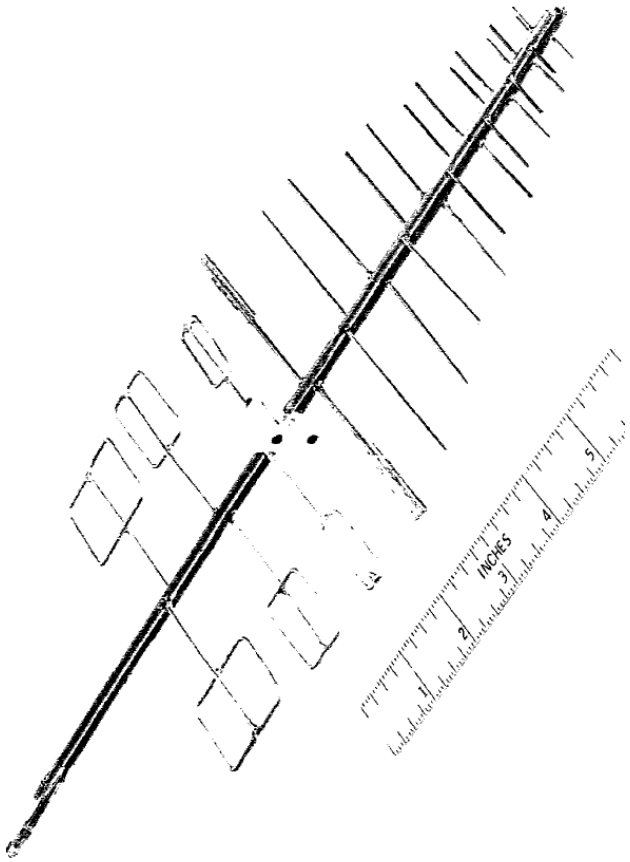

Figure 1.7. Hybrid LPDA consisting of size-reduced and full-sized elements (Kuo 1970).

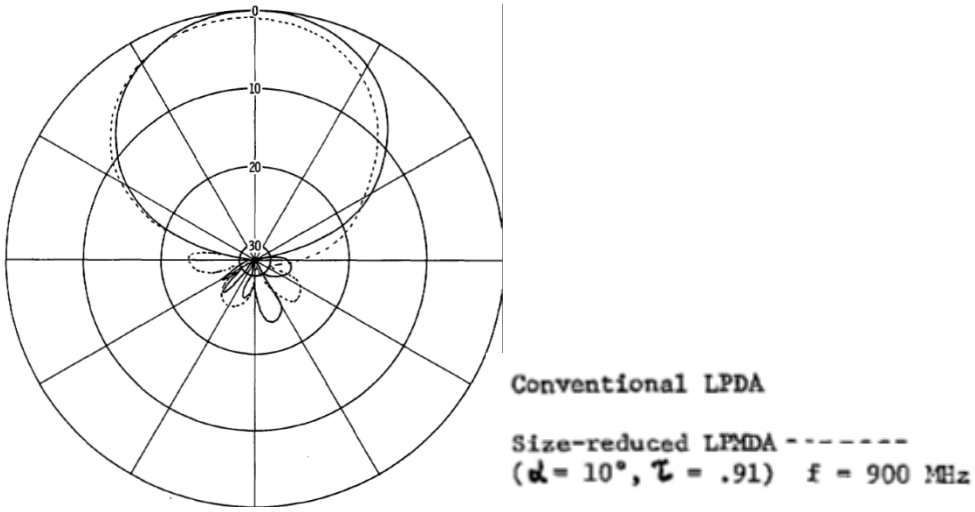

Figure 1.8. E-plane radiation pattern of size-reduced LPDA and conventional LPDA (Kuo 1970).

In another study, Koch-shaped (fractal) dipoles are implemented in an LPDA, and it resulted in a 12 % area reduction in comparison to a printed, conventional LPDA with λ/2 dipole elements (Anagnostoul, et al. 2008). Figure 1.9 shows the prototype of the Koch LPDA alongside a conventional printed LPDA.

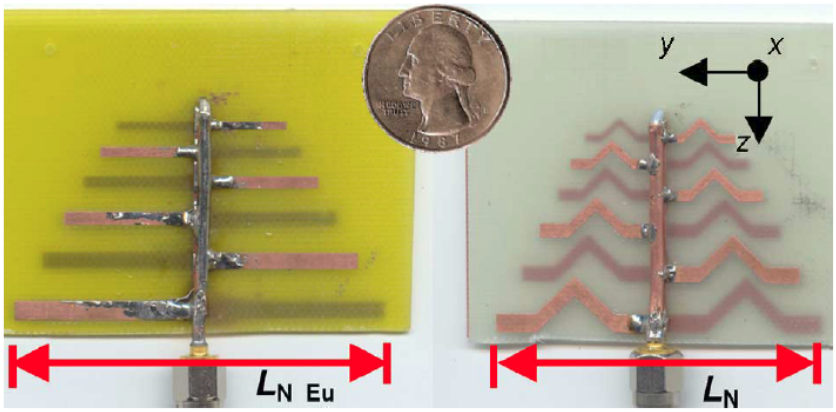

Figure 1.9. Printed LPDA (left) and Koch LPDA (right) (Anagnostoul, et al. 2008).

A size-reduced LPDA with cylindrical-hat covers on dipoles achieved a 31 % length reduction of the longest dipole element in the LPDA, and the overall area was reduced to 50 % of that of a conventional LPDA with λ/2 dipole elements (Jardon-Aguilar, et al. 2010). The prototype is shown in Figure 1.10.

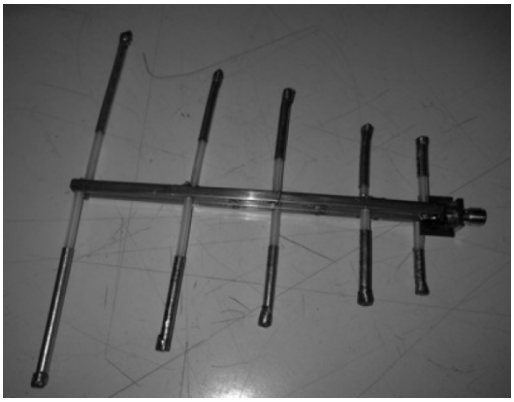

Figure 1.10. Cylindrical hat LPDA prototype (Jardon-Aguilar, et al. 2010).

Recently, a size-reduced LPDA using T-top loaded dipole elements was presented (Rhodes and Lim 2013). The half-wavelength dipoles on a conventional LPDA are replaced with 0.8 *kr* T-top loaded dipoles, which have the same impedance bandwidth as half-wavelength dipoles. The resulting LPDA is shown in Figure 1.11, alongside a conventional LPDA utilizing half-wavelength dipole elements. With this simple yet effective method of miniaturization of the LPDA, a possibility of making a circularly polarized top-loaded LPDA is feasible.

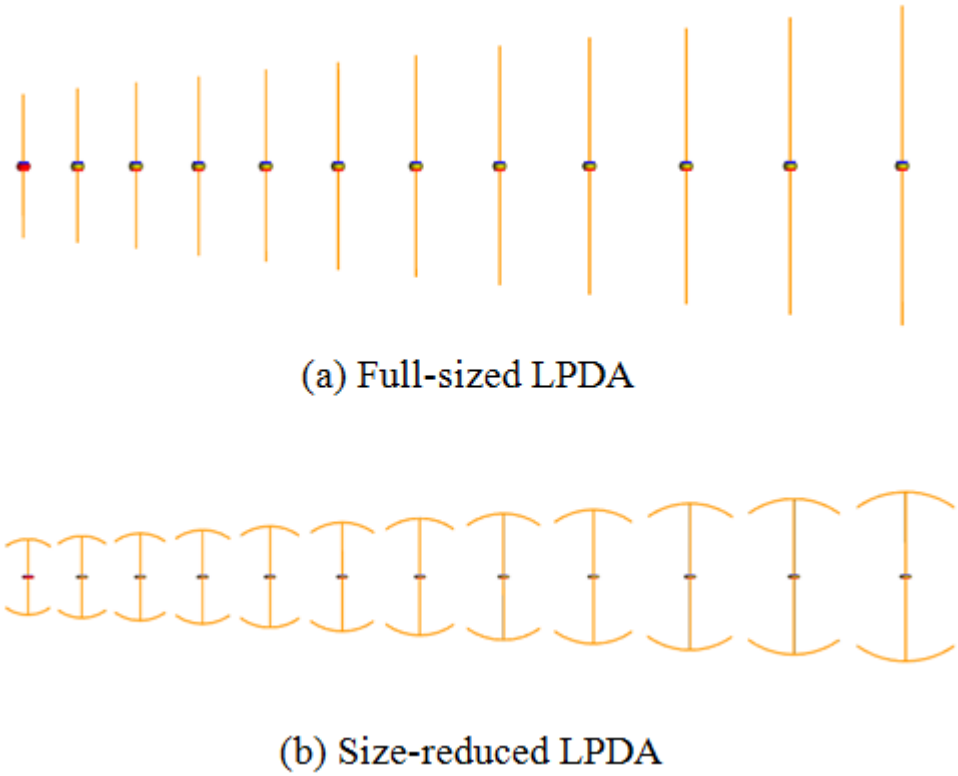

Figure 1.11. Conventional LPDA (a) and T-top loaded size-reduced LPDA (b) (Rhodes and Lim 2013).

1.4 Objectives of Thesis

The main objective of this thesis is to design and analyze electrically small, circularly polarized novel antenna designs. Various methods of antenna miniaturization are described, with the main focus on top-loading as an efficient method of miniaturization. With existing knowledge of advancements and techniques of antenna design, two new antenna designs are created. The analysis of the simulation results of the implementation of top-loading in these two new antenna designs is presented and discussed.

1.5 Overview of Thesis

Chapter 2 presents a planar, circularly polarized cross dipole antenna design. The most basic form of the design, a crossed dipole (Bolster 1961), creates circular polarization by unequal length dipoles connected by a single feed. This design is made into a planar design and then top-loaded to achieve miniaturization.

Chapter 3 introduces a newer design of a previous miniaturized LPDA (Rhodes and Lim 2013). The design follows the same concept as the T-top loaded LPDA, but is applied to a circularly polarized LPDA that consists of two feeds with a 90° phase shift between each feed. The result is a circularly polarized compact LPDA that maintains a similar impedance bandwidth and average gain compared to that of a conventional LPDA.

Lastly, Chapter 4 provides a summary of the novel antenna designs and their significance in this thesis. Future work and possible improvement upon these designs is also presented.

CHAPTER 2

THE DESIGN OF AN ELECTRICALLY SMALL, CIRCULARLY POLARIZED PLANAR CROSS DIPOLE

2.1 Introduction

In this chapter, a new planar antenna design is discussed. A circularly polarized, planar cross dipole antenna is presented with an electrical size, *kr*, of 0.65. The antenna starts off as a cross dipole (Bolster 1961). The cross dipole is created as a planar antenna and then miniaturization is performed in several steps. Miniaturization of the antenna is first achieved by employing top-loading on both ends of the crossed dipoles, and then adding further arms onto the end of the top-loaded sections. Short stubs are implemented to boost the reduced radiation resistance that accompanies the reduced size of the antenna. Unlike other CP planar antennas, the proposed antenna is printed on a single layer, allowing for low cost production. A single-point feed is used for the generation of CP. The antenna is printed on Rogers RT/Duroid 5880, having a dielectric constant, ε_r, of 2.2, and a thickness of 3.2 mm. The antenna operates at 912 MHz, where the maximum realized gain of the antenna is 1.37 dBic and the axial ratio is below 3 dB. Simulations of the design are compared to measurement data to verify the antenna's capability in the real world.

2.2 Antenna Design

The geometry of the proposed antenna is presented in Fig. 2.1. The principle structure of the antenna is a crossed dipole (Bolster 1961). In this previous design, two dipoles are placed perpendicular to one another and are connected by a central feed point. One dipole is slightly longer than the other, allowing CP to be generated with a single-point feed. Figure 2.2 shows the geometry of the crossed dipole, and Figure 2.3 shows the resulting axial ratio of the design, which achieves circular polarization (axial ratio less than 3 dB). Utilizing this base design, circular polarization can be achieved without the use of special external means, such as a matching circuit or phasing lines. From closer examination of the currents on the antenna, the main radiators can be seen to have maximum current 90° out of phase with each other, which is the reason for CP.

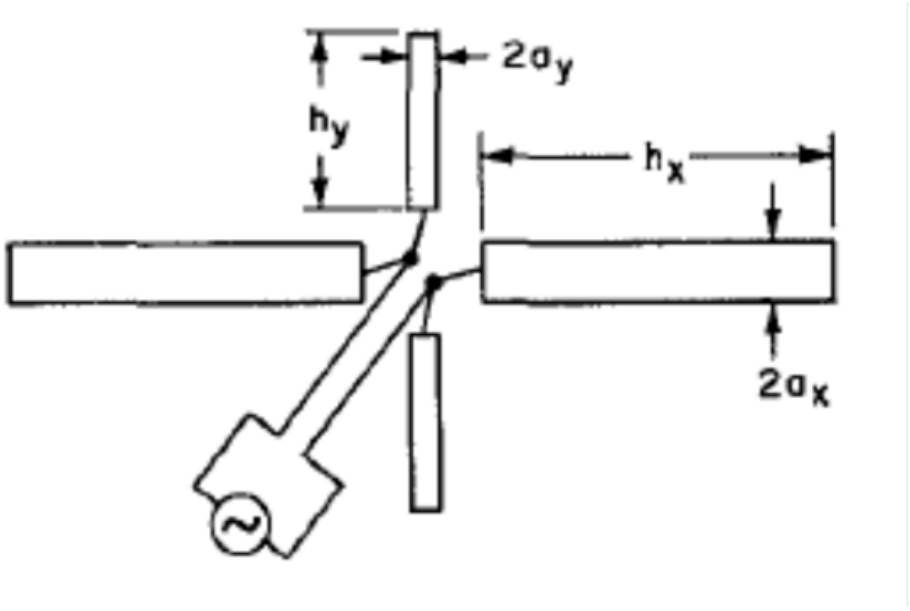

Figure 2.1. Crossed dipole antenna design (Bolster 1961).

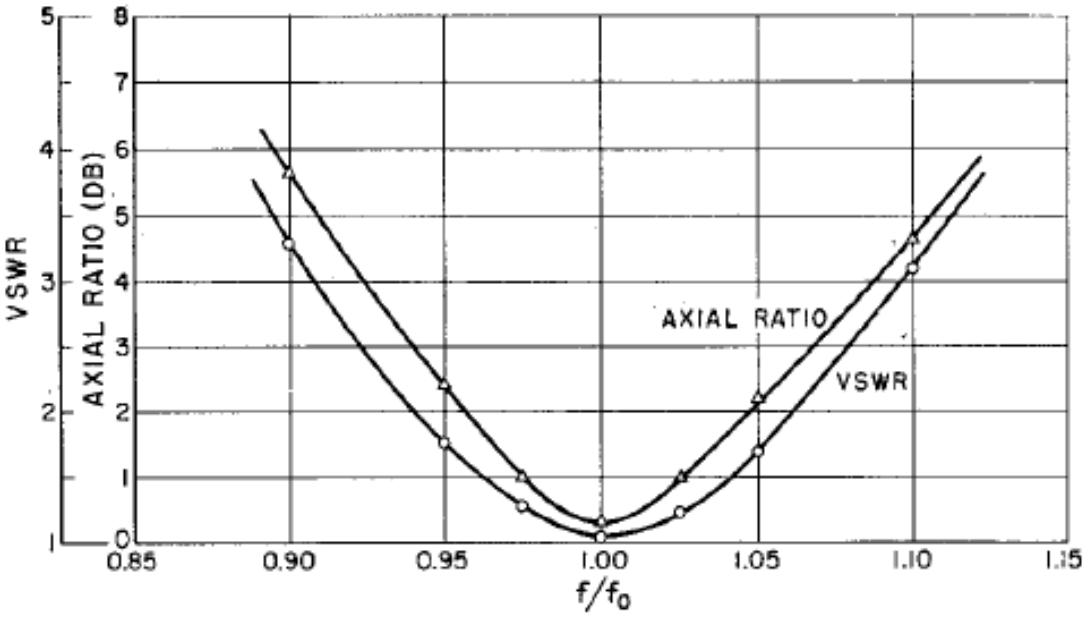

Figure 2.2. Crossed dipole antenna frequency vs. axial ratio (Bolster 1961).

From this base design, the size of the antenna is reduced by utilizing a two-arm, top loading structure on both ends of each dipole. Top-loading is useful in reducing antenna size, as shown in the antenna design in Figure 2.3 (Lim, Rogers and Ling 2006). This design employs a spherical helix top-loaded design, which is able to achieve miniaturization to a size of a 0.19 *kr*.

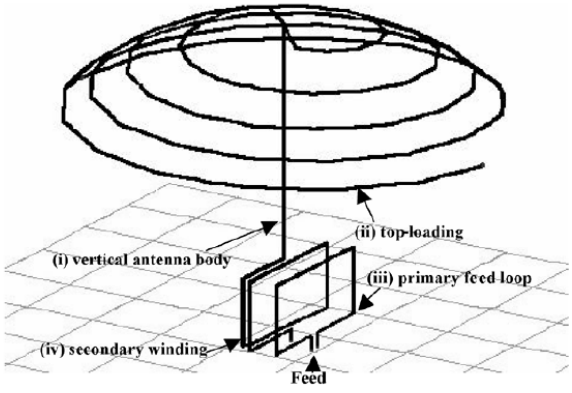

Figure 2.3. Electrically small, tunable antenna with spherical helix top-loading (Lim, Rogers and Ling 2006).

The electrical length of each dipole is easily changed by varying the length of the top loading structure. As an antenna's electrical size becomes smaller and smaller, the general trend is that radiation resistance drops. Therefore, two identical short stubs are added between orthogonal dipole elements, boosting the low radiation resistance that occurs due to the antenna's electrically small size. The antenna is printed on Rogers RT/Duroid 5880 that has a dielectric constant, ε_r, of 2.2, and a thickness of 3.2 mm.

The evolution of the design process of the antenna can be summarized and observed through simulation, in Figure 2.4. The first design starts at the basic cross dipole. The cross dipole is a wire antenna. The simulated realized gain is found to be 2.02 dBic (a normal dipole is typically ~2.14 dB), and the axial ratio is 0.92 dB. The size of antenna structure is an electrical size, *kr*, of 1.71. The cross dipole is then created as a planar design with an offset on the horizontal radiator to accompany the feed. The design is printed on Rogers RT 5880. The realized gain is simulated to be 2.09 dBic and axial ratio 2.41 dB, with an electrical size, *kr*, of 1.56. By planarizing the cross dipole, the realized gain is about the same and axial ratio is still under 3 dB. In order to make the antenna electrically small ($kr < 1$), top-loading is then employed onto the planar cross dipole design. To maintain symmetry of the top-loading in a circle, the feed is repositioned to be in line so that the vertical and horizontal dipoles are lined up with the feed. The resulting performance is a slight drop in realized gain to a value of 1.65 dBic, an improved axial ratio of 0.92 dB, and an electrical size, *kr*, of 0.79. At this size, the design is considered electrically small, but further size reduction would be better. So, two arms are added onto each of the top-loading structures. Initially, the axial ratio is maintained under 3 dB but the realized gain is poor due to impedance mismatch caused

by low radiation resistance. This is fixed by using T-matching stubs across the feed, shorting the horizontal and vertical dipoles on each side, as done in previous research (Yu and Lim 2012). The result is an electrical size, *kr*, of 0.65. Further size reduction results in poor performance, so this size is adequate for the design. The final design is further analyzed in simulation to view the characteristics of the antenna.

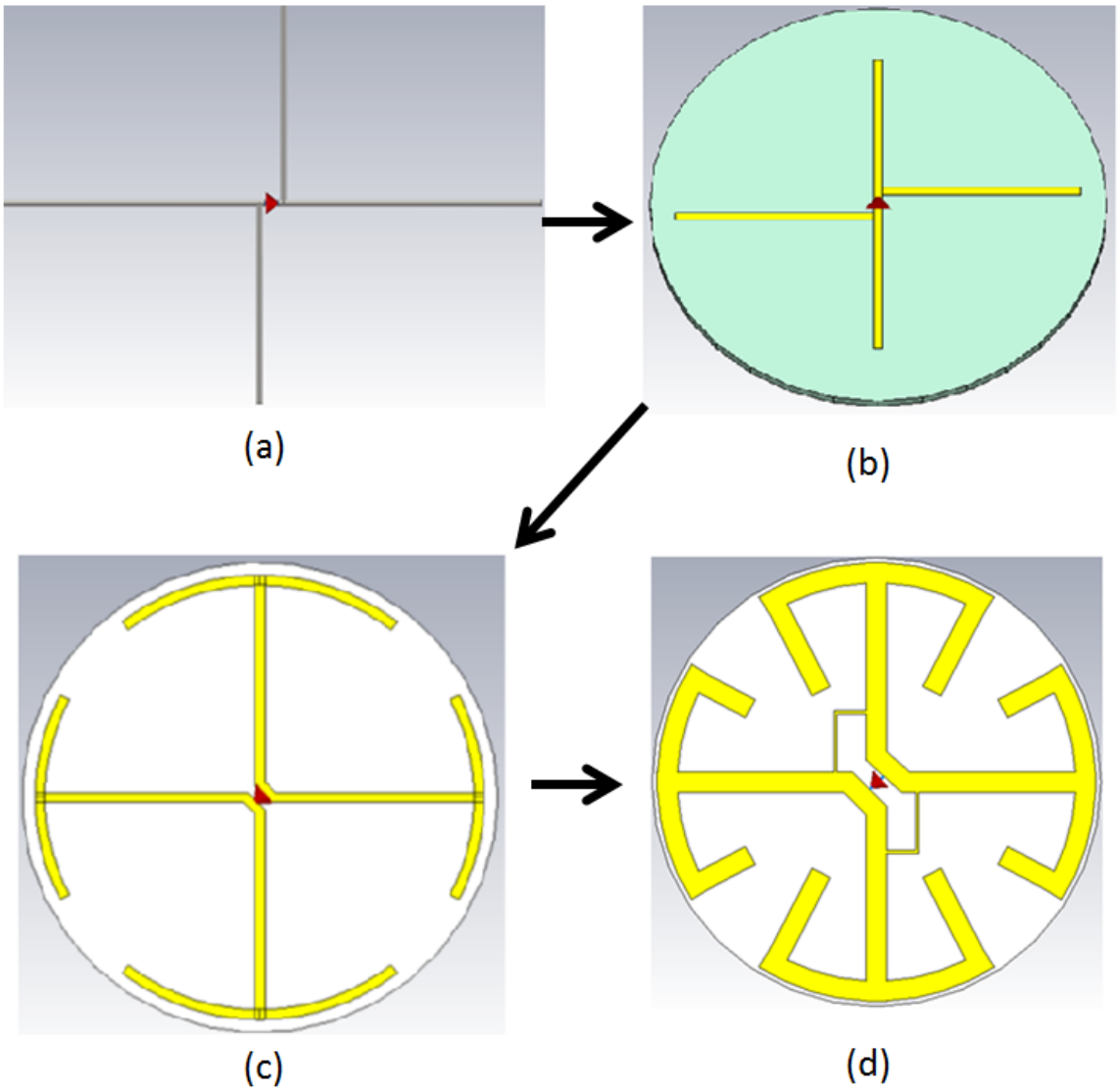

e,

(b) planar crossed dipole, (c) addition of top-loading, (d) addition of two arms on top-loading and T-matching stubs.

2.3 Simulation and Measurement Results

The dimensions of the antenna were optimized with a genetic algorithm (GA) to maximize realized gain (RG) in the zenith direction and minimize axial ratio (AR) at a frequency of 912 MHz. The diameter of the antenna is 6.8 cm (0.2λ) and the total electrical size, *kr*, is 0.65. Figure 2.5 shows the simulated S_{11} of the antenna. The optimized antenna has a 10-dB bandwidth of 5.6 % (881 – 932 MHz), the minimum S_{11} is -23 dB occuring at a frequency of 894 MHz. The AR vs. Frequency of the antenna is shown in Figure 2.6. The 3-dB AR bandwidth is 1.5 % (908 – 922 MHz). The minimum AR is 0.96 dB at 915 MHz. Next, the AR pattern at 912 MHz is plotted in Fig. 2.7. The 3-dB AR beamwidth is 61° in the XZ plane and 101° in the YZ plane. Finally, the realized gain pattern of the antenna is depicted in Figure 2.8. The maximum realized gain is 1.37 dBic and the 3-dB beamwidth is 141°. The radiation efficiency of the antenna is 98% at 912 MHz.

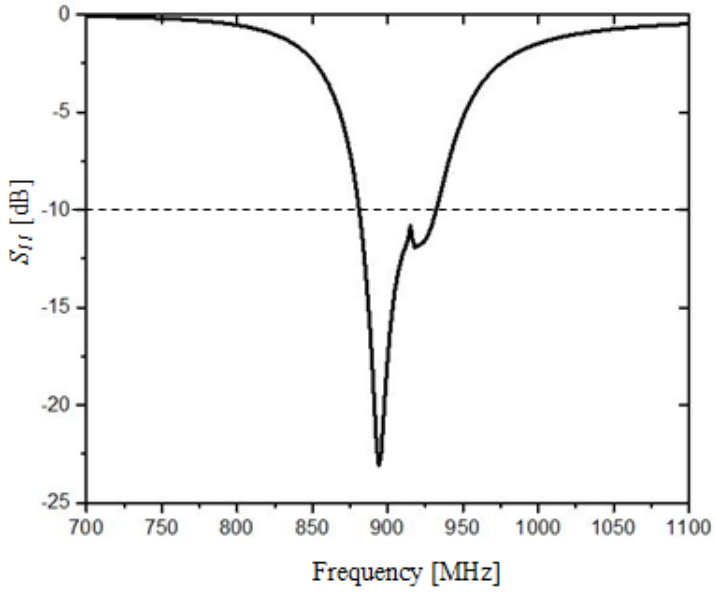

Figure 2.5. S_{11} vs. frequency of the PCD antenna design.

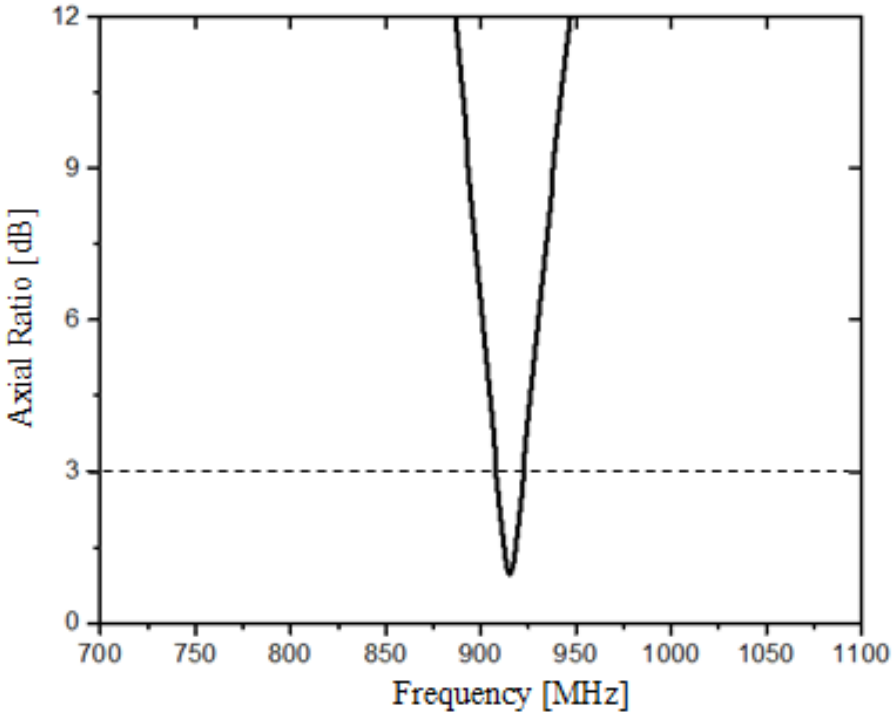

Figure 2.6. Axial ratio vs. frequency of the PCD antenna design.

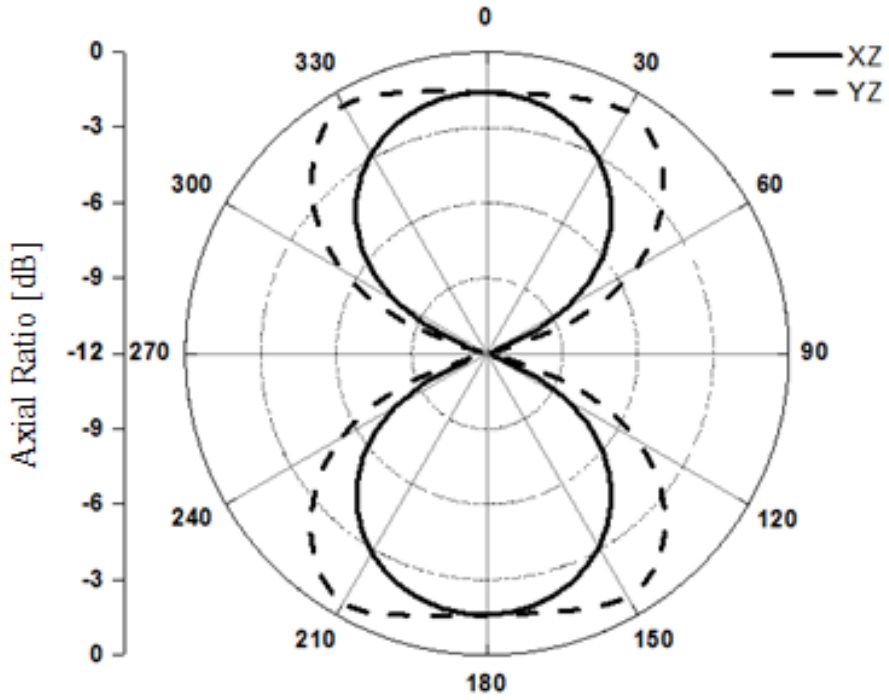

Figure 2.7. Inverted axial ratio vs. angle of the PCD antenna design.

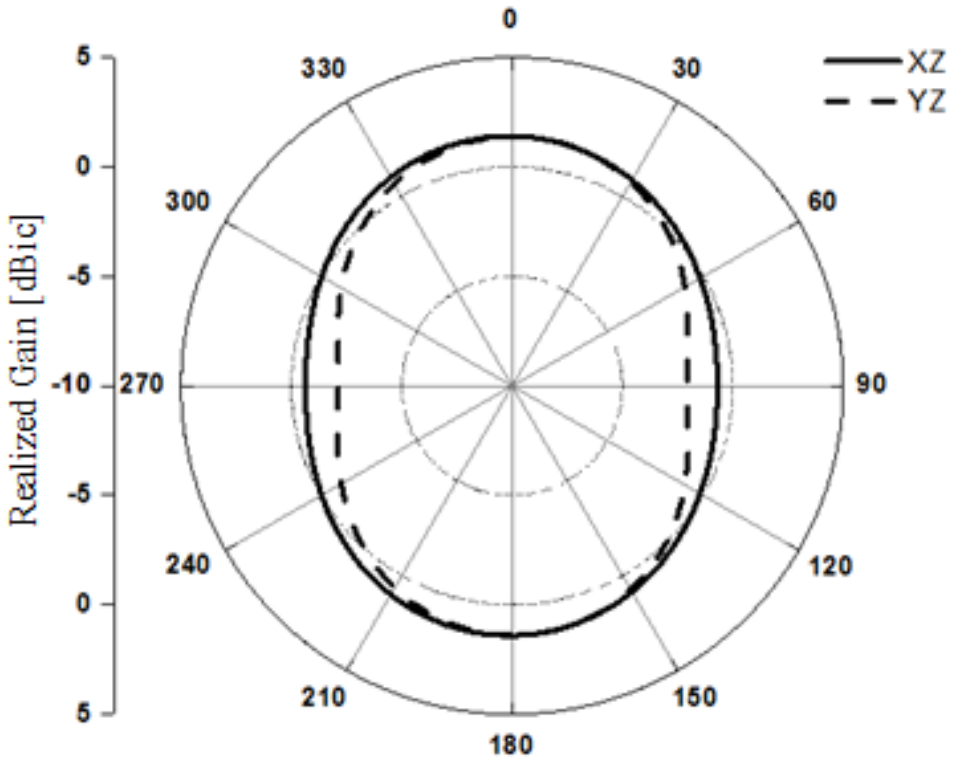

Figure 2.8. Realized gain radiation pattern of the PCD antenna design.

The next step is to verify simulations with measurement. In preparation for measurement, the antenna is remade at a different frequency than 912 MHz. The chosen frequency is 1.5 GHz, so that the horn antenna can be used for a reference antenna. The horn antenna used in the measurements can be seen in Figure 2.8. The horn antenna has a pyramidal shape with a rectangular mouth. The horn is linearly polarized and the orientation of the horn is vertical in the photo. The benefit of using the horn is that it operates on a wide band, from 1 GHz up to 2 GHz. The measurement is performed using an antenna rotator in conjunction with a network analyzer and a computer. The data is recorded on the computer from the analyzer while the antenna is rotated.

Figure 2.9. Pyramidal horn antenna.

S_{11} and axial ratio vs. frequency curves were also recorded and plotted alongside simulation results. The S_{11} vs. frequency curve is shown in Figure 2.10. The double dip pattern can be seen, which signifies circular polarization in a cross dipole antenna design. A slight frequency shift is apparent, due to small fabrication error. An S_{11} value below -10 dB represents 90% power transfer from the system to the antenna, which is the standard for a well-matched antenna. The minimum measured S_{11} of the antenna occurs at 1.46 GHz with a value of -18 dB. The double dip pattern can be seen, with the operating frequency at the dip being slightly shifted down to 1.48 GHz.

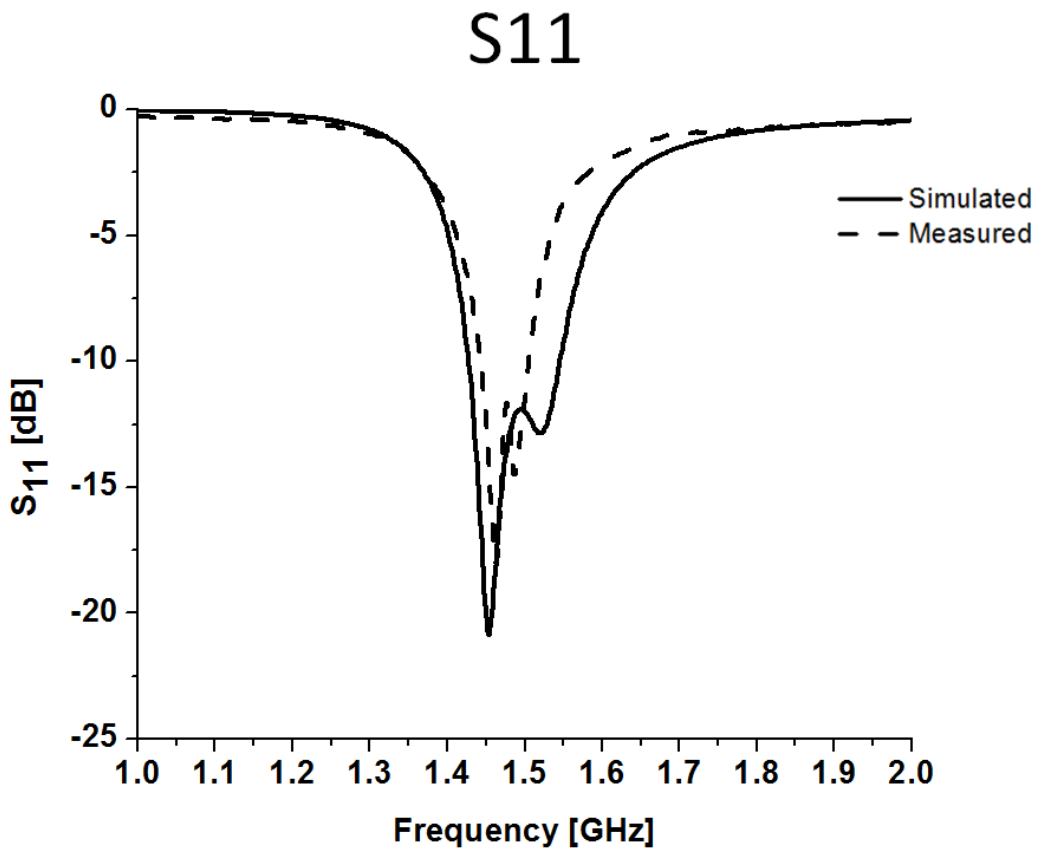

Figure 2.10. Simulated and measured S_{11} vs. frequency.

For a circularly polarized antenna such as this one, the method of recording farfield data is slightly different than the measurement for a linearly polarized antenna. The planar cross dipole antenna has to be rotated 4 times: on the XZ theta plane, XZ phi plane, YZ theta plane, and YZ phi plane. Comparing these four radiation patterns to the simulation should result in a close comparison, with the total XZ and YZ calculated pattern from the measurements matching up well to the simulation total patterns. Also, the S_{11} and axial ratio should match that of the simulation. At a frequency of 1.48 GHz,

the four radiation patterns (XZ/YZ theta, XZ/YZ phi) can be seen in Figures 2.11 through 2.14.

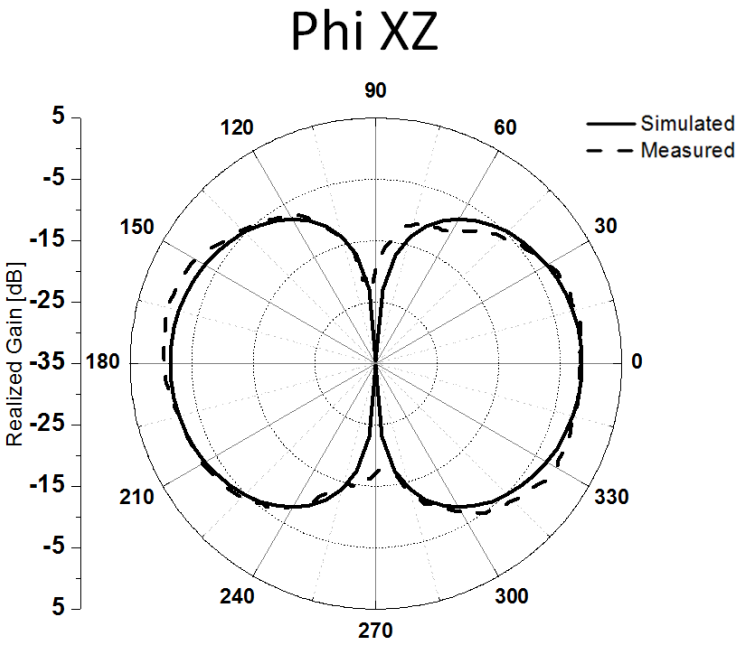

Figure 2.11. Simulated and measured phi XZ radiation pattern.

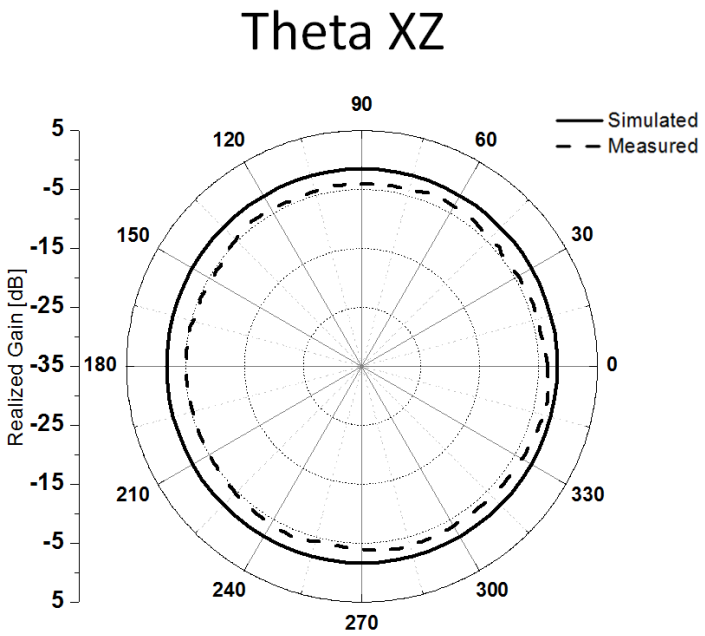

Figure 2.12. Simulated and measured theta XZ radiation pattern.

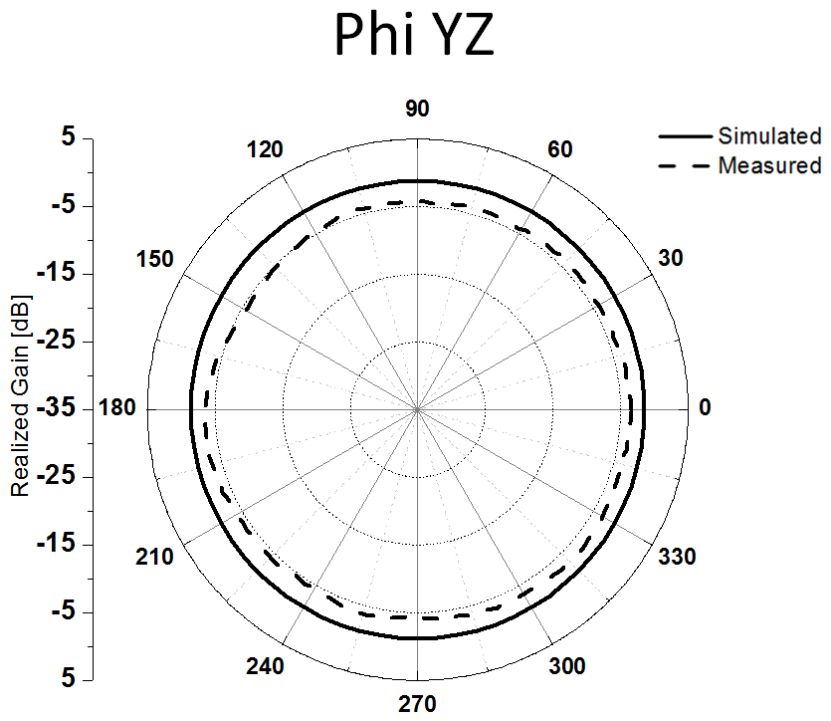

Figure 2.13. Simulated and measured phi YZ radiation pattern.

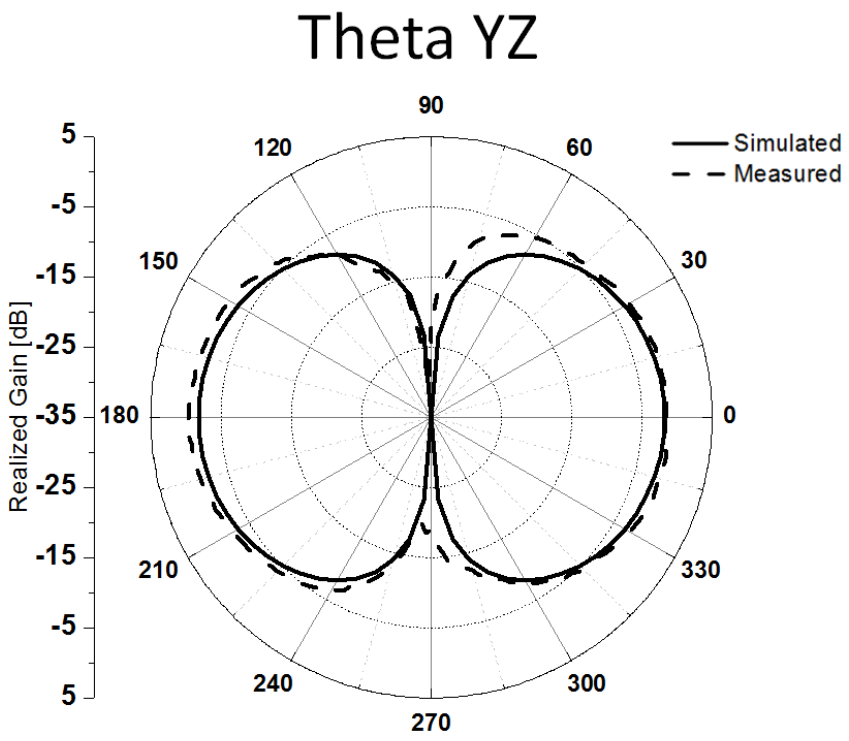

Figure 2.14. Simulated and measured theta YZ radiation pattern.

The measurements match up fairly well in all measurements. XZ corresponds to the orientation of the antenna as shown in Figure 2.4(d), and YZ corresponds to the antenna in the XZ position but rotated 90° clockwise. The phi XZ and theta YZ patterns match up well between measurement and simulations, with only small variation. Theta XZ and phi YZ patterns match well, except for roughly a 2 dB drop in the measured results. To calculate the total patterns, the formula used is:

$$Total = \sqrt{(\phi\text{-}pol.)^2 + (\theta\text{-}pol.)^2}\,, \tag{2}$$

which has to be applied to XZ and YZ separately. By calculating the total pattern using this equation, the measured XZ and YZ patterns shown in Figure 2.15 and Figure 2.16, respectively, are plotted along with the corresponding simulation results.

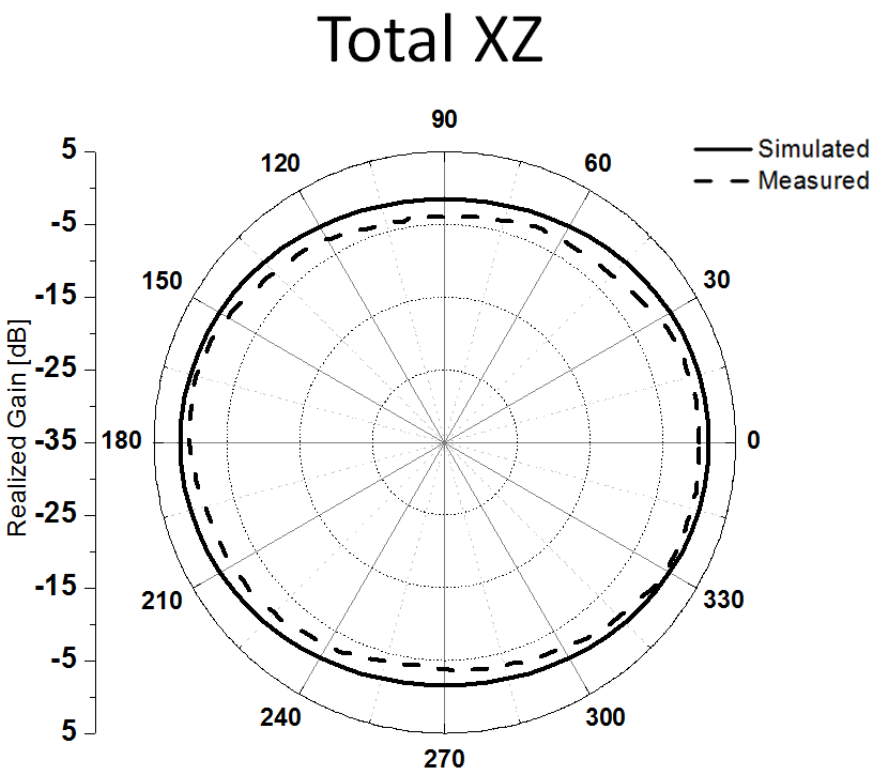

Figure 2.15. Simulated and measured total XZ radiation pattern.

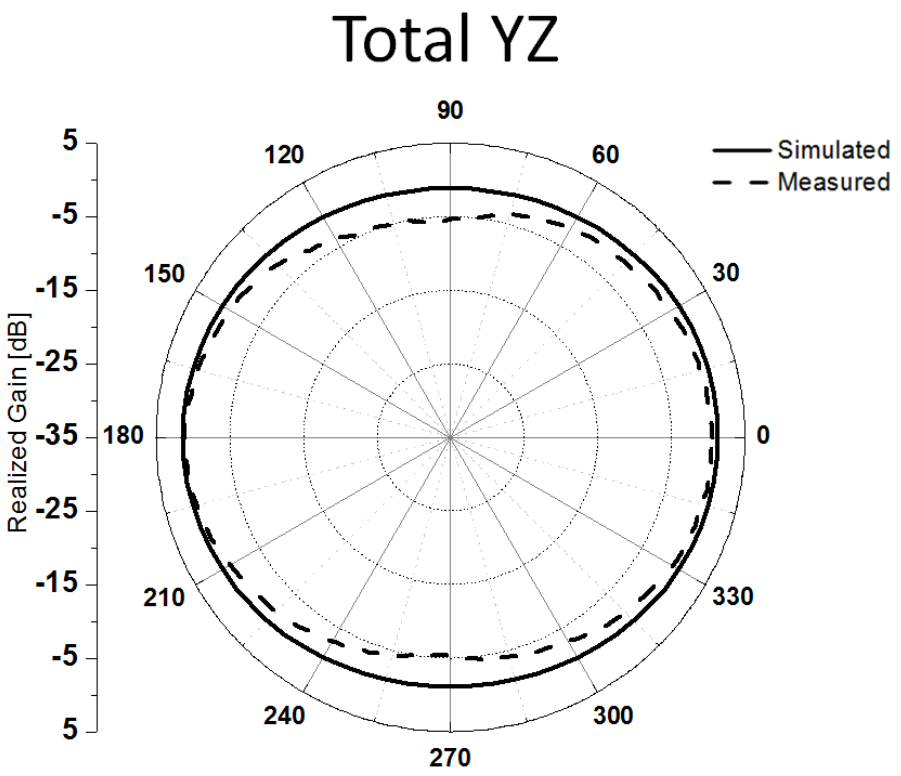

Figure 2.16. Simulated and measured total YZ radiation pattern.

The measured realized gains total patterns match well with simulations. The directions in which the antenna is to be used (0° and 180° in the polar plots) matches very well in magnitude with the simulations, with the 90° and 180° directions being a couple dB lower than simulation results. The simulated and measured axial ratio vs. frequency plot in Figure 2.17 shows the minimum occurring at 1.5 GHz on the simulation, and 1.48 GHz on the measurement, as expected.

Discrepancies in measurement vs. simulation data can be described by the antenna creation and measurement process. In simulation the antenna is fed through an ideal method, a discrete port. In the fabrication of the antenna, not only must a simple SMA connector as a feed be attached, but a quarter-wavelength balun must also be attached to

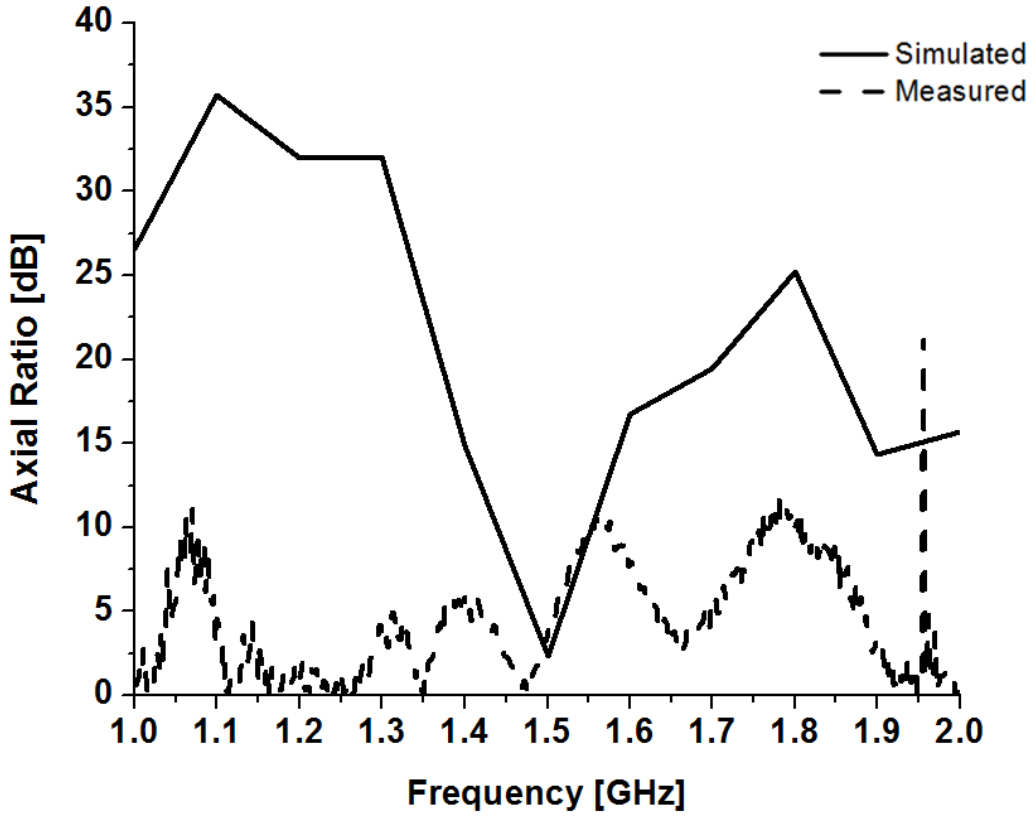

Figure 2.17. Simulated and measured axial ratio vs. frequency.

the antenna. The balun is pictured in figure 2.18, attached to the antenna. The balun is necessary when a balanced antenna like a dipole is connected to an unbalanced system, like the network analyzer. In short, it works by drawing a cancelling current from the center of the coax to the outer shell. The result is an S_{11} and thus radiation pattern that isn't significantly affected by reverse currents in the transmission line, which can vary by objects being close to the transmission line. The balun also does not affect the impedance of the antenna. However, it is naturally a narrowband phenomenon as it is frequency-dependent, so the antenna results aren't accurate outside of the frequency area in which the balun is created (1.5 GHz in this case).

Figure 2.18. Planar cross dipole prototype.

2.4 Summary

A novel electrically small, circularly polarized planar cross dipole antenna design is presented and analyzed. The design accomplishes the goal of miniaturization by employing top-loading to reduce the electrical size of the antenna while maintaining good performance. The problem of low radiation resistance is solved by utilizing T-matching

to provide an increase in impedance. The simulations performed in CST:MWS using a genetic algorithm. A prototype of the antenna is fabricated using a quarter-wavelength balun, and measurement results are recorded. Simulation and measurement results are compared and discussed, and are found to be in good agreement.

CHAPTER 3

DESIGN OF A CIRCULARLY POLARIZED, T-TOP LOADED COMPACT LOG-PERIODIC DIPOLE ARRAY

3.1 Introduction

In this chapter, a circularly polarized, T-top loaded compact log-periodic dipole array is presented. This novel design is based off of that of the T-top loaded LPDA (Rhodes and Lim 2013). However, the concept of top-loading the LPDA is applied to a full-size conventional circularly polarized LPDA. The goal is to maintain circular polarization, an S_{11} below -10 dB, and a high realized gain across the frequency band of interest. First, a background of the top-loaded LPDA is discussed. Next, the CP top-loaded compact LPDA is presented with simulation results. Finally, further simulations are performed in order to prepare the antenna design for fabrication.

3.2 Background

In this section, a compact log-periodic dipole array (LPDA) is presented. The individual dipole elements of a conventional LPDA are miniaturized by employing T-top loading to reduce the length from λ/2 to λ/4 (50% reduction). Then the different-sized, T-top loaded dipoles are combined to produce an LPDA with comparable impedance bandwidth and realized gain across the same frequency band of that of a λ/2 element LPDA. The compact LPDA is shown to have a 65 % area reduction of that of the λ/2

element LPDA design while maintaining an S_{11} below -10 dB across the frequency band of interest from 1 to 1.5 GHz.

3.2.1 Introduction

In this section, a new compact LPDA is suggested to reduce the overall area of the LPDA by implementing T-top loaded dipoles instead of λ/2 dipole elements. First, gradual size reduction of a T-top loaded dipole is applied, and the best design is selected based on the smallest size possible to maintain comparable impedance bandwidth and realized gain to that of a λ/2 dipole. In the T-top design, a shape that is conformal to a sphere is chosen to maximize the volume of the antenna in the '*kr*' sphere ('*k*' is the wave number and '*r*' is the radius of the smallest sphere that encloses antenna.) defined in Wheeler (Wheeler 1947). Since impedance bandwidth of a λ/2 dipole is far below the Wheeler-Chu limit at its size of 1.6 '*kr*' (Chu 1948), the electrical size of the dipole can be reduced with T-top loading while still maintaining the similar impedance bandwidth of the λ/2 dipole. Next, after designing a T-top loaded dipole, six elements of differently scaled T-top loaded dipoles are combined to achieve a compact LPDA to cover the frequency band of 1 to 1.5 GHz. The optimization of the compact LPDA is performed by using a genetic algorithm (GA).

The compact LPDA consists of six elements, and has the wire radius fixed at 1.63 mm (AWG # 8). The simulation results of the compact LPDA are discussed and compared to that of a λ/2 element LPDA. Finally, the compact LPDA antenna prototype is fabricated and measured.

3.2.2 Antenna Geometry

As shown in Figure 3.1, four T-top loaded dipoles are designed at 1.25 GHz with different electrical sizes, *kr*, of 1.6, 1.2, 0.8, and 0.6, respectively. Since the wave number *k* is fixed due to the fixed center frequency of 1.25 GHz, the electrical size, *kr,* is mainly controlled by *r*. In this way, the electrical size of the antenna is directly controlled by the top-loading length. A comparison between the impedance bandwidth of various sized dipoles is shown in the simulated S_{11} curves of the antennas (Figure 3.2(a)). It is observed that the 10-dB impedance bandwidth is nearly identical in all antennas except for that of the 0.6 *kr* dipole. Due to the impedance mismatch, a poor realized gain value can be expected of the 0.6 *kr* dipole as shown in the realized gain plot of the top-loaded dipoles in Figure 3.2(b). Thus, the 0.6 *kr* dipole is too small to be utilized in an LPDA using this top-loaded design. From these results, an LPDA using λ/4, or 0.8 *kr*, T-top loaded dipole elements is viable, enabling the construction of a compact LPDA with comparable performance to that of the λ/2 element LPDA. Further reduction of the T-top loaded element results in poor impedance matching.

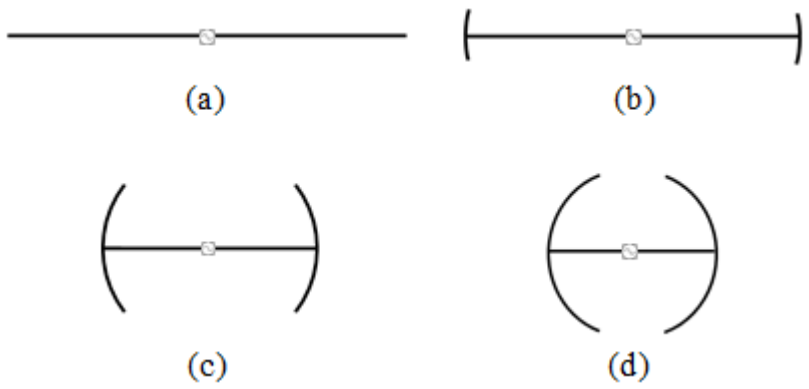

Figure 3.1. Geometry of the (a) 1.6 *kr* dipole, (b) 1.2 *kr* dipole, (c) 0.8 *kr* dipole, and (d) 0.6 *kr* dipole.

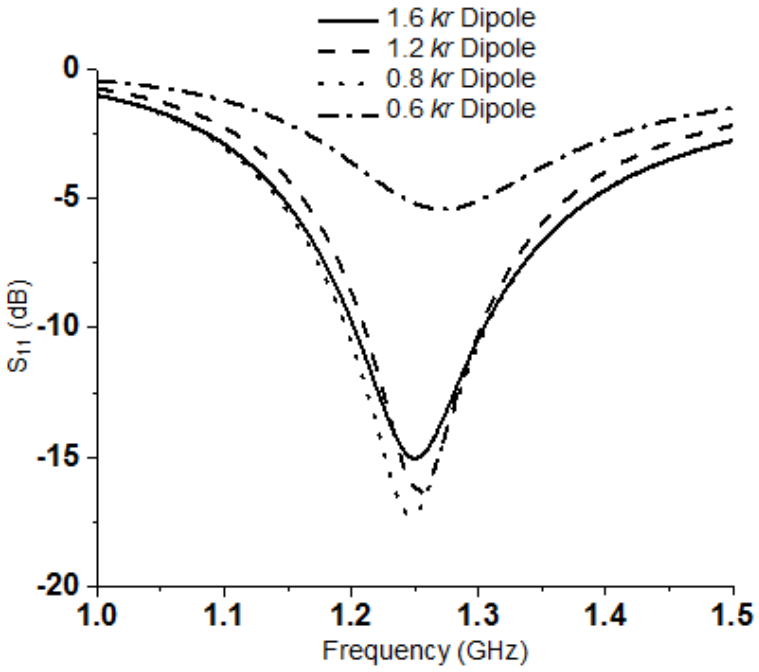

(a)

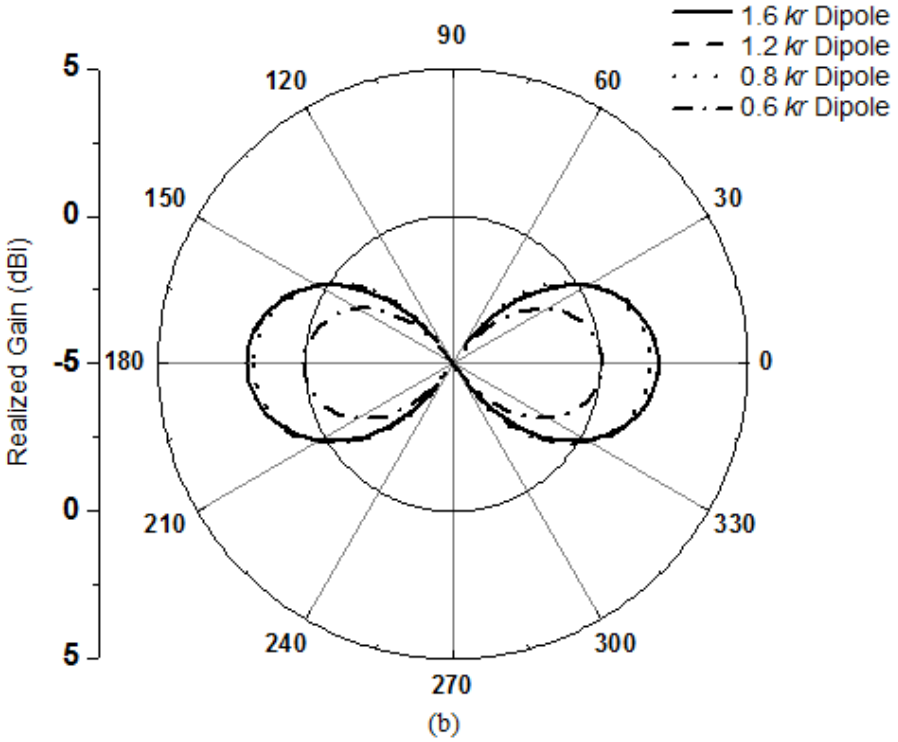

(b)

Figure 3.2. Simulated (a) S_{11} and (b) realized gain of the 1.6 *kr*, 1.2 *kr*, 0.8 *kr*, and 0.6 *kr* dipoles.

With the 0.8 *kr* dipole being the best selected design, a compact LPDA can be created consisting of 0.8 *kr* dipoles. For comparison to a conventional LPDA, a λ/2 element LPDA is also created at the same frequency band. Both LPDAs consist of 6 elements and have an operating frequency from 1 to 1.5 GHz. Fig. 3 shows the geometry of the λ/2 element and compact LPDAs. On the compact LPDA, the top-loading lengths (the arc length from one end to the other end) of each individual element are fixed to be 9 % longer than the half of the vertical segment of the dipole. This ratio of top-loading length to vertical dipole segment is employed to maintain a *kr* of 0.8 for each top-loaded dipole element.

The compact LPDA is created in FEKO and optimized using a GA, with goals of impedance bandwidth below -10 dB across the entire band and maximum realized gain toward the shortest dipole direction. The cost function of the GA can be defined by

$$cost = (w_1 \times (TG - G)) + (w_2 \times (|TS| - |S|)) , \quad (3)$$

where w_1 is a weight of 1, TG is the target realized gain of 10 dBi, G is the average realized gain across the entire frequency band, w_2 is a weight of 2, TS is the target S_{11} at -10 dB, and S is the average S_{11} across the frequency band of interest. Optimization parameters consist of each spacing length from one element to the next and length of each vertical dipole segment. The optimization goals of the compact LPDA were to maintain an S_{11} below -10 dB and to maximize average realized gain across the frequency band of 1 to 1.5 GHz. A similar λ/2 element LPDA is also optimized with the same goals

and parameters. The feed for each LPDA is located at the smallest element, between the positive and negative transmission lines.

As expected, the compact LPDA dipole elements are roughly half of the length of the λ/2 dipole elements. The spacing between elements is significantly changed, with the greatest element spacing on the compact LPDA being nearly 60% of the greatest spacing on the λ/2 element LPDA. The calculated area of the λ/2 element LPDA is 151.9 cm^2 and the calculated area of the compact LPDA is 52.6 cm^2, resulting in a 65% area reduction.

3.2.3 Simulation Results

With a 50 Ω reference impedance, the λ/2 element LPDA is able to maintain an S_{11} below -10 dB across the majority of the frequency band of interest, as seen in Figure 3.3. The compact LPDA manages to maintain an S_{11} below -15 dB for the entirety of the frequency band, verifying that the 0.8 *kr* dipole elements have no negative effect on impedance bandwidth by using them instead of λ/2 dipole elements.

The simulated realized gain of both LPDAs is similar from 1 to 1.5 GHz, as illustrated in Figure 3.4. The maximum realized gain achieved is 6.91 dBi for the λ/2 element LPDA and 7.51 dBi for the compact LPDA. The maximum difference in realized gain is 0.71 dB and occurs at 1.16 GHz. Figure 3.5 shows the simulated elevation realized gain radiation patterns for both LPDAs at four evenly spaced frequencies within the frequency band from 1 to 1.5 GHz. The radiation patterns are very similar, with the compact LPDA being slightly more directive in the forward direction (90°).

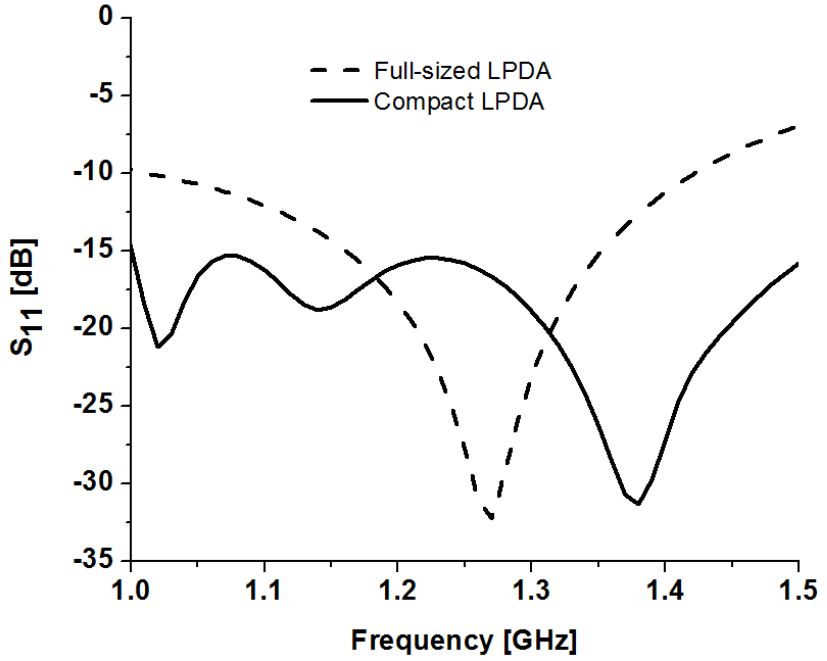

Figure 3.3. Simulated S_{11} of the full-sized and compact LPDA.

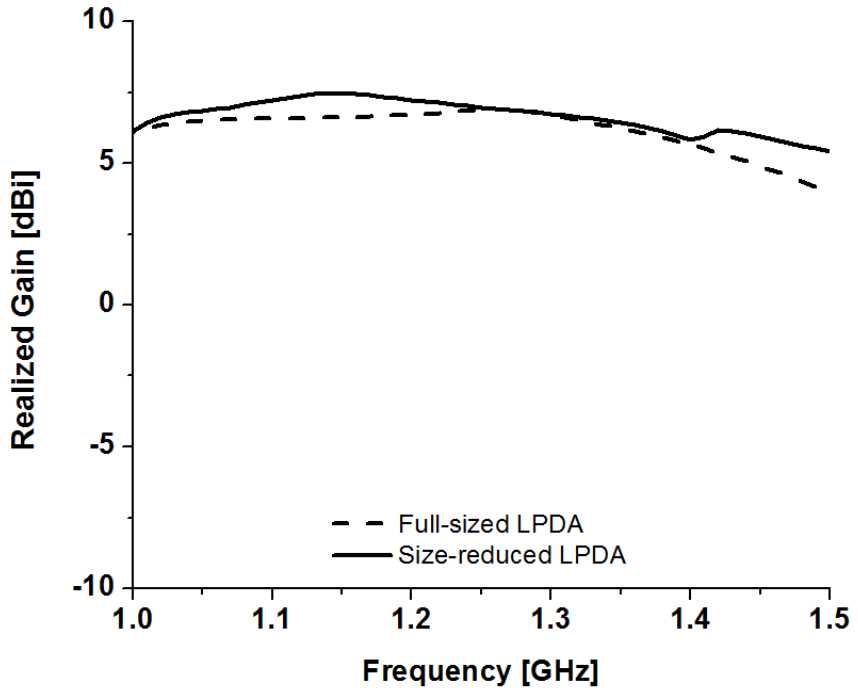

Figure 3.4. Simulated realized gain vs. frequency of the full-sized and compact LPDA.

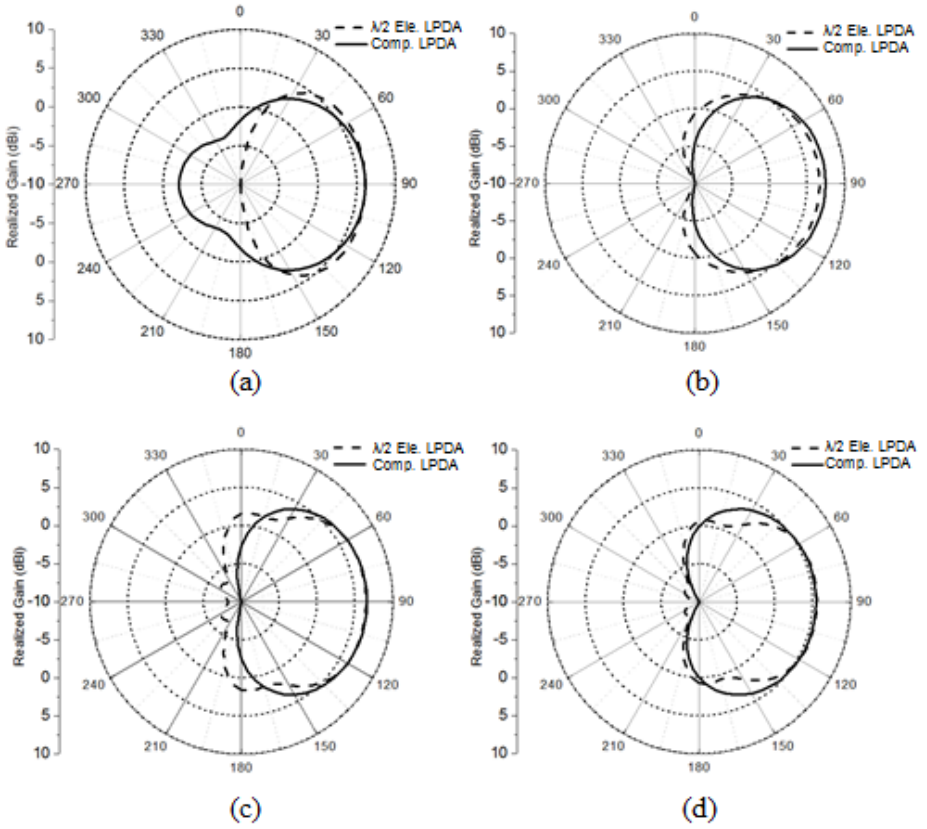

Figure 3.5. Simulated elevation realized gain patterns of the λ/2 element and compact LPDAs at: (a) 1.00GHz, (b) 1.16GHz, (c) 1.33GHz, (d) 1.50GHz.

Afterwards, measurement results were taken and compared to the simulation results. Measurements were in good agreement with simulations. The fabricated prototype is shown in Figure 3.6. The transmission lines of the LPDA are separated by balsa wood to prevent them from shorting out and for providing stability in the structure. Balsa wood is used because of its low dielectric constant, ε_r, 1.3. Compared to the dielectric constant of air ($\varepsilon_r = 1$), the balsa wood can provide stability without having a significant effect on the antenna.

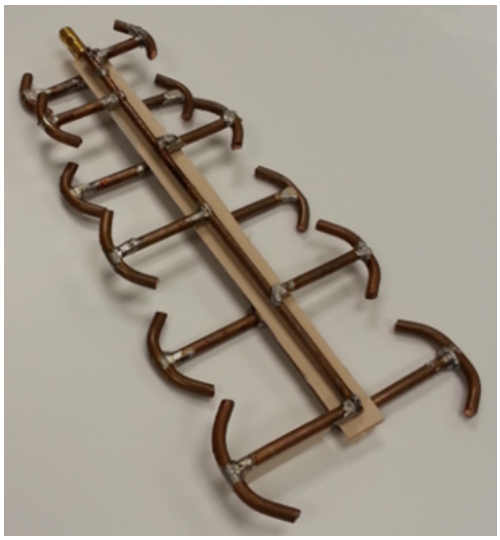

Figure 3.6. Compact LPDA prototype.

3.3 Initial Antenna Design and Simulation Results

Using the method of T-top loading on the LPDA, it is possible to create a compact circularly polarized LPDA by top-loading a circularly polarized LPDA in the same fashion. The first step is to use a working CP LPDA, which is done by using a pre-made CP LPDA in the software Antenna Magus. The 11-element design can be seen in Figure 3.7. The construction of the antenna is basically a combination of two orthogonal LPDAs. The design contains two feeds on the end of the antenna with the smallest elements, and two 200 Ω loads on the end of the antenna with the largest elements. The two feeds are supposed to be fed 90° out of phase to produce circular polarization. The antenna's reference impedance is 100 Ω, which is typical for this kind of design. If a 50 Ω impedance was desired, two options can be explored: modifying the antenna (such as the boom) or designing the antenna for 200 Ω and utilizing a 4:1 balun. The resistive load on the end of the antenna opposite the feed points is used to suppress spikes in the reflection coefficient.

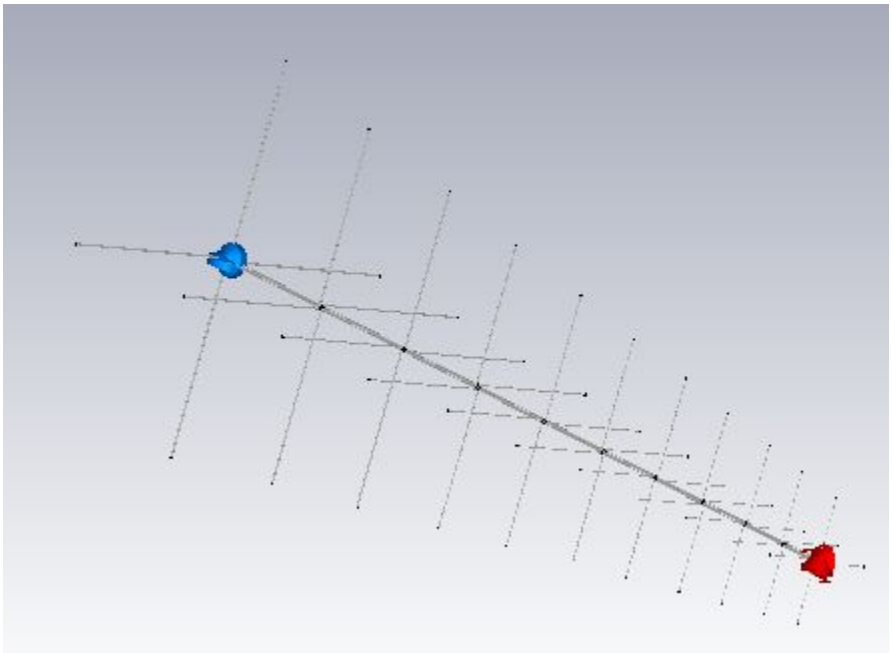

Figure 3.7. Full-size CP LPDA created through Antenna Magus.

Simulations conducted on the design in CST:MWS reveal the radiation characteristics and impedance of the antenna. Figure 3.8 depicts the S_{11}, which shows a good resonance below -10 dB from 0.76 to 2.5 GHz. The wide frequency range can be attributed to the fact that the CP LPDA consists of 11 elements which allows for wider bandwidth due to an increased number of dipole elements at varying frequencies. The realized gain vs. frequency curve can be seen in Figure 3.9. The peak realized gain occurs at 1.5 GHz with a value of 8.33 dBic. A 3D perspective of this gain value at 1.5 GHz can be seen in Figure 3.10. The antenna is shown to be directive toward the smallest element. In Figure 3.11, the axial ratio is seen to be very low across the entire frequency band, with a maximum value of 0.81 dB at the upper end of the frequency band. Due to the 90° phase shift between the two ports, circular polarization is expected to occur as it does across the entire frequency band.

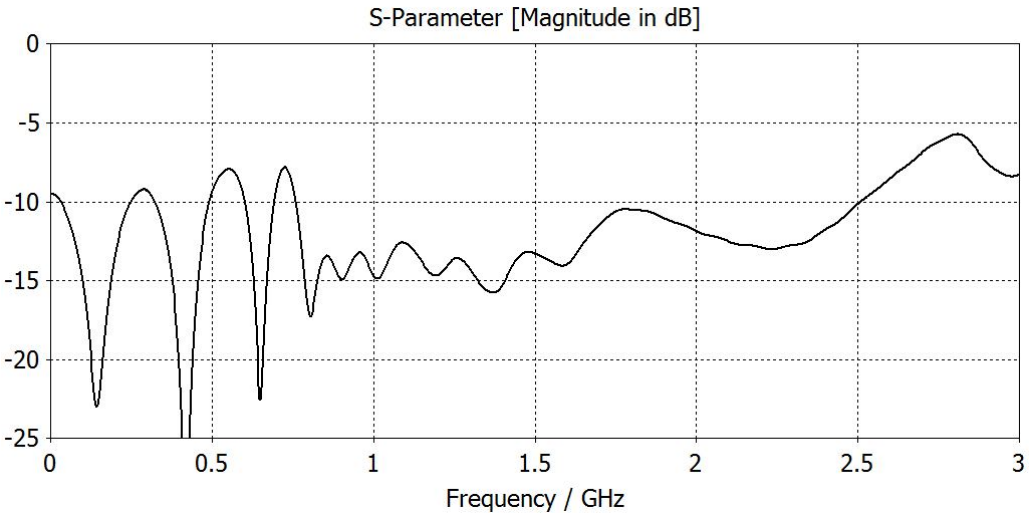

Figure 3.8. Full-size CP LPDA simulated S_{11}.

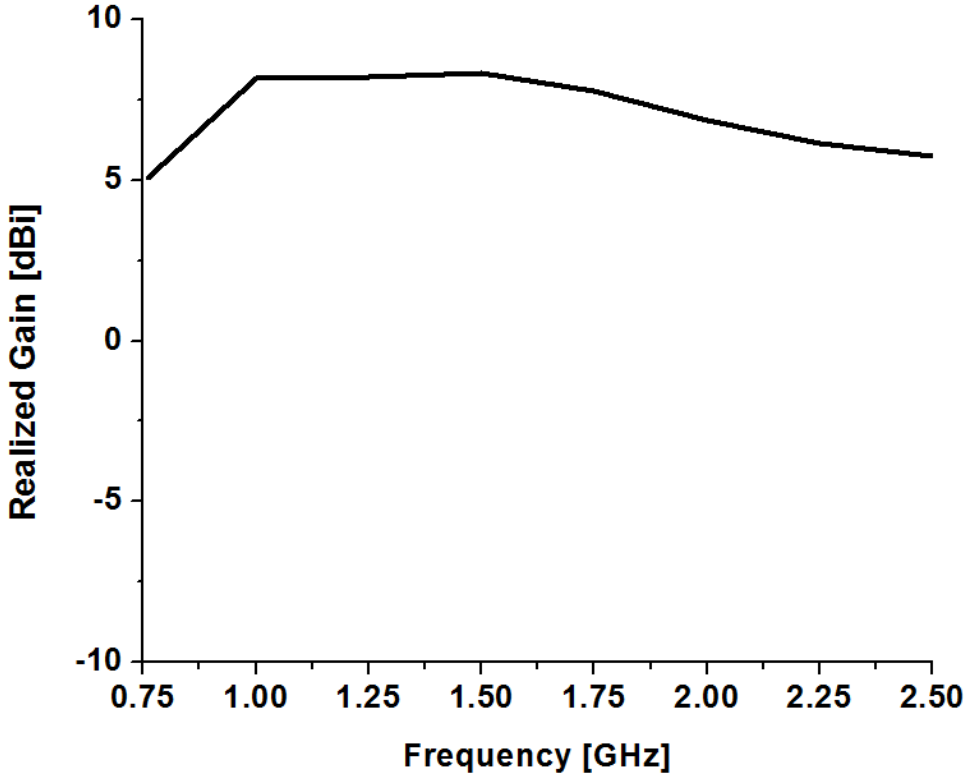

Figure 3.9. Full-size CP LPDA simulated realized gain vs. frequency.

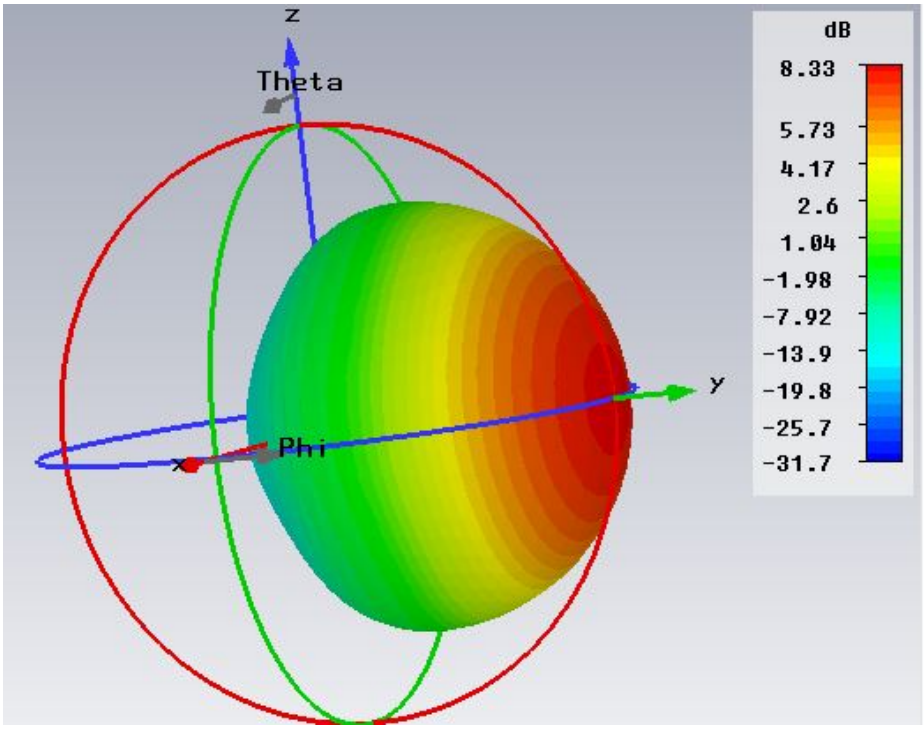

Figure 3.10. Full-size CP LPDA simulated 3D realized gain pattern at 1.5 GHz.

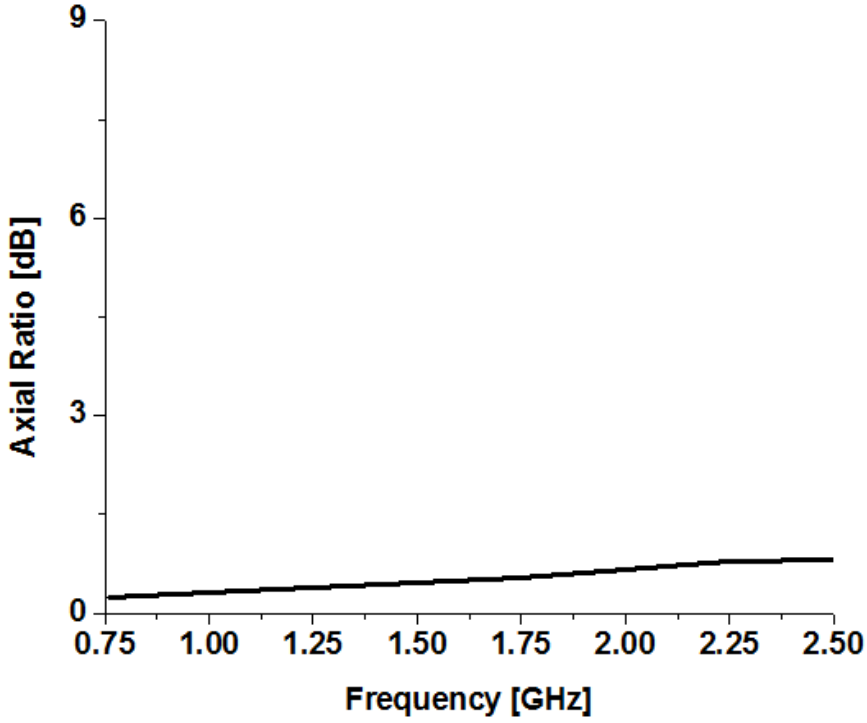

Figure 3.11. Full-size CP LPDA simulated axial ratio vs. frequency.

The next step is to add top-loading to the dipole elements of the full-size CP LPDA. To do this, the element lengths must be reduced to compensate for the top-loading. As in the linear compact LPDA, the CP LPDA full-size dipole elements must be reduced in length by one-half, and then a T-top loading structure applied with a length dependent on the length of dipole element. The top-loading structure follows a curve whose angle is 62.28° and radius is the length of its vertical segment (which is one-half of a dipole). Since the wire radius of every element in the LPDA is dependent on the scale factor, every element has a different wire radius. The top-loading structure for each element will have a wire radius that matches the wire radius of that individual element. Afterwards, the result is the design whose geometry is depicted in Figure 3.12. The top-loading reduces the overall width of the antenna by one-half, making the design compact.

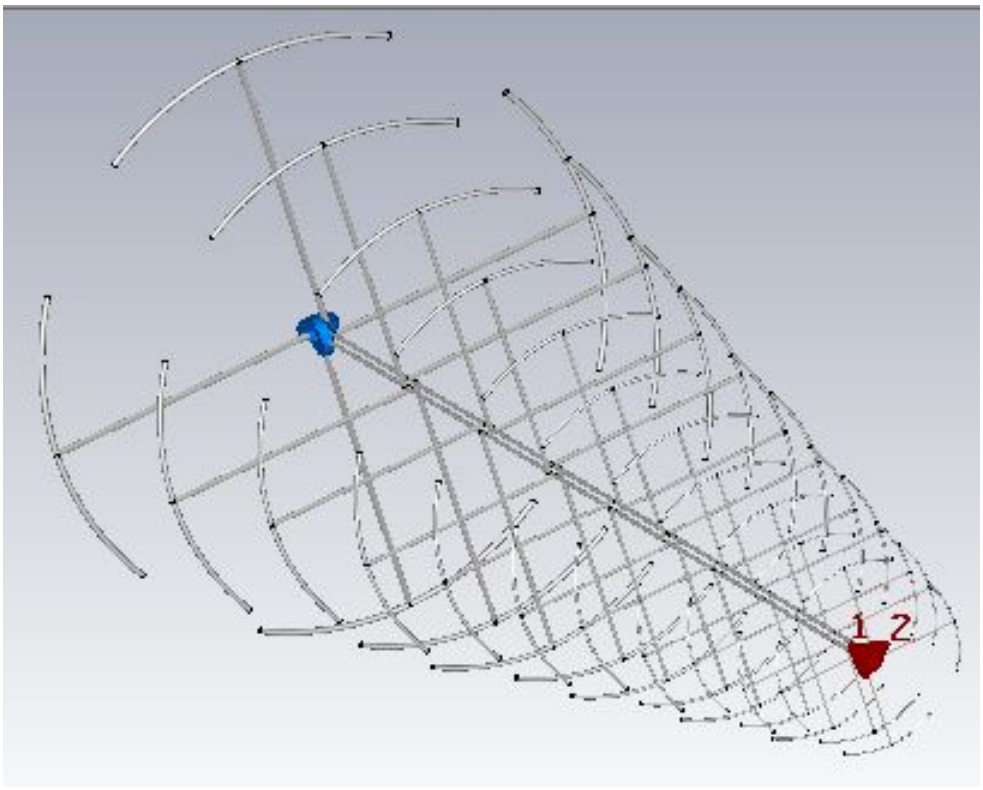

Figure 3.12. Compact CP LPDA geometry.

The simulated S_{11} of the compact CP LPDA is shown in Figure 3.13. A slight frequency shift to the right can be observed, but the wide band is still maintained. The bandwidth (-10 dB) spans from 0.88 GHz to 2.67 GHz. Figure 3.14 shows a slight drop in realized gain, but still maintains a value of 6.75 dBic at the peak at 1.25 GHz. Axial ratio follows the same correlation in that a slight increase is noticed, but the maximum value of 1.04 dB at the upper end of the frequency band is still well below the 3 dB requirement for circular polarization. This axial ratio vs. frequency curve can be seen in Figure 3.15. Just as the full-sized CP LPDA simulation was performed, the characteristic impedance of the antenna in the simulation is 100 Ω instead of the typical 50 Ω, and a 90° phase shift is implemented into one of the feeds. From this simulation data, it can be concluded that T-top loading is an effective method of miniaturization that can maintain circular polarization, impedance bandwidth, and realized gain values from the initial CP LPDA.

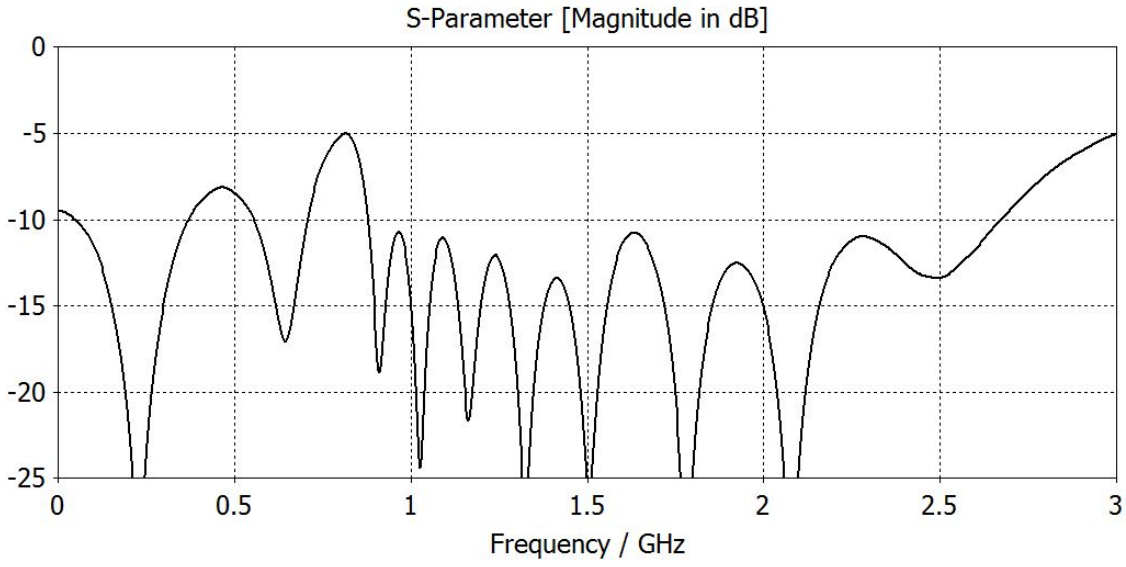

Figure 3.13. Compact CP LPDA simulated frequency vs. S_{11}.

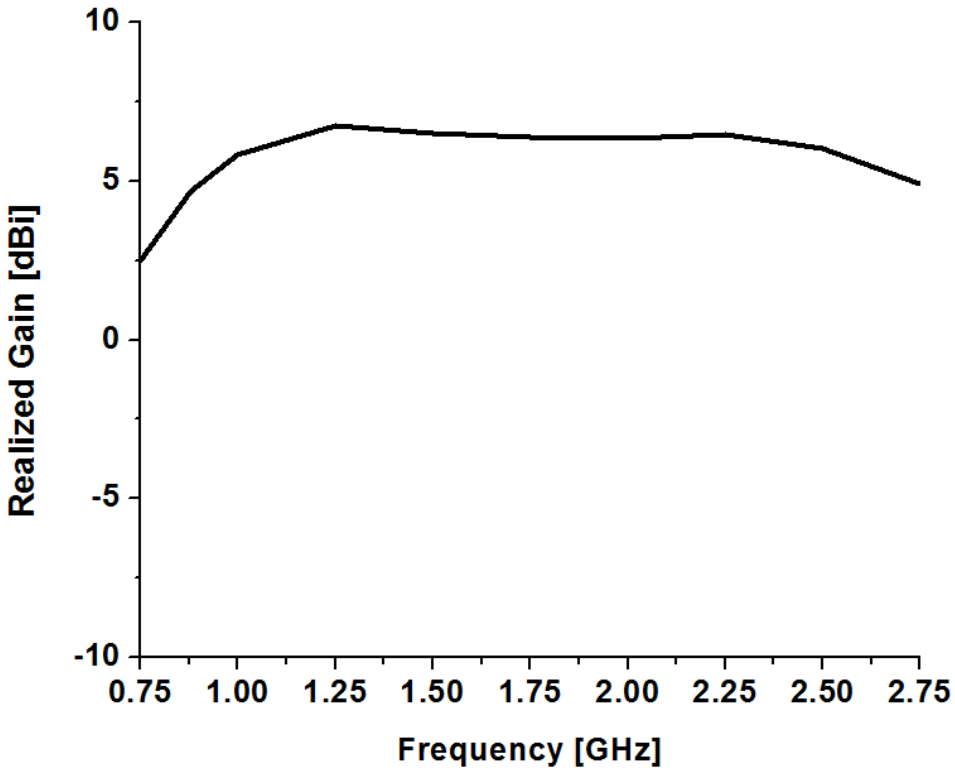

Figure 3.14. Compact CP LPDA simulated frequency vs. realized gain.

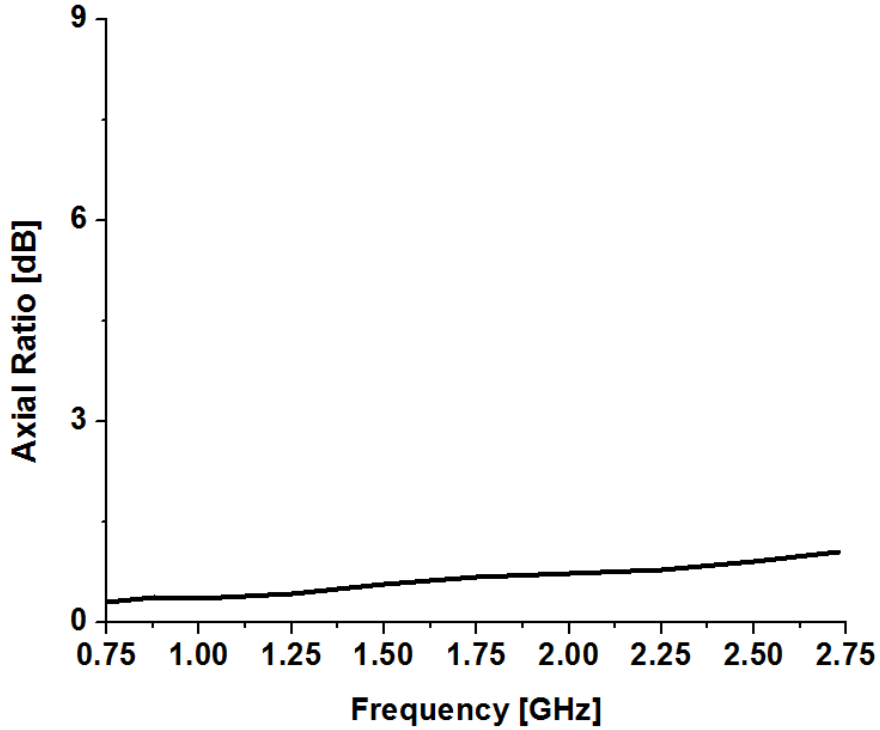

Figure 3.15. Compact CP LPDA simulated frequency vs. realized gain.

3.4 Further Simulations for Antenna Fabrication

After confirmation of the working method of the T-top loaded compact CP LPDA, the next step in the antenna design process is to make a similar design that is easier to fabricate. An 11-element design with varying wire radius on every element will be very difficult to make and more susceptible to fabrication error. Too many elements make the fabrication take much longer and requires more soldering. The varying wire radii make fabrication nearly impossible due to unavailability of the wire size; the wire sizes will not fall into common wire sizes on the American wire gauge size chart.

3.4.1 Reduction in Number of Elements

The first idea to facilitating fabrication of the compact CP LPDA is to reduce the number of elements in the antenna. This can be easily accomplished by simply taking the 11-element design and cutting off the largest five elements to produce a 6-element design. This should result in the same performance results of the full-size CP LPDA but with a portion of the lower frequency cut off. The 6-element design geometry can be seen in Figure 3.16, and the top-loaded compact design version of this can be seen in Figure 3.17.

The simulation of both the 6-element full-size CP LPDA and the 6-element compact CP LPDA are performed simultaneously and the results compared to each other and to previous design results. Figures 3.18 and 3.19 show the S_{11} curves of the 6-element full-size and 6-element compact CP LPDAs, respectively. The full-size results show a reduction in the lower portion of the frequency bandwidth, as compared to the 11-element full-size design. The new impedance bandwidth range spans from 1.32 to 2.46 GHz. However, the top-loaded 6-element design produces poor impedance matching.

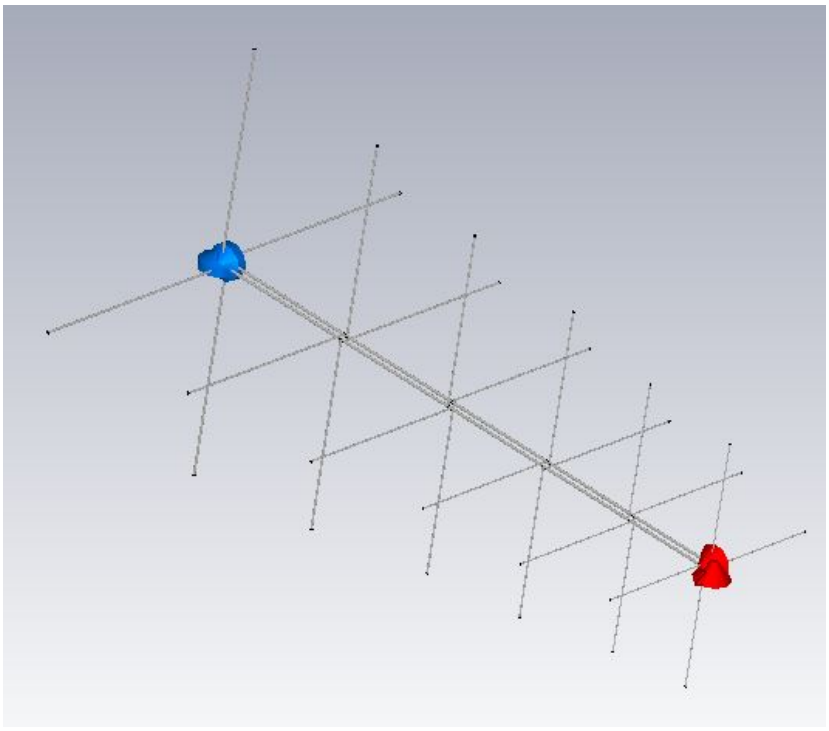

Figure 3.16. Full-size CP LPDA 6-element design.

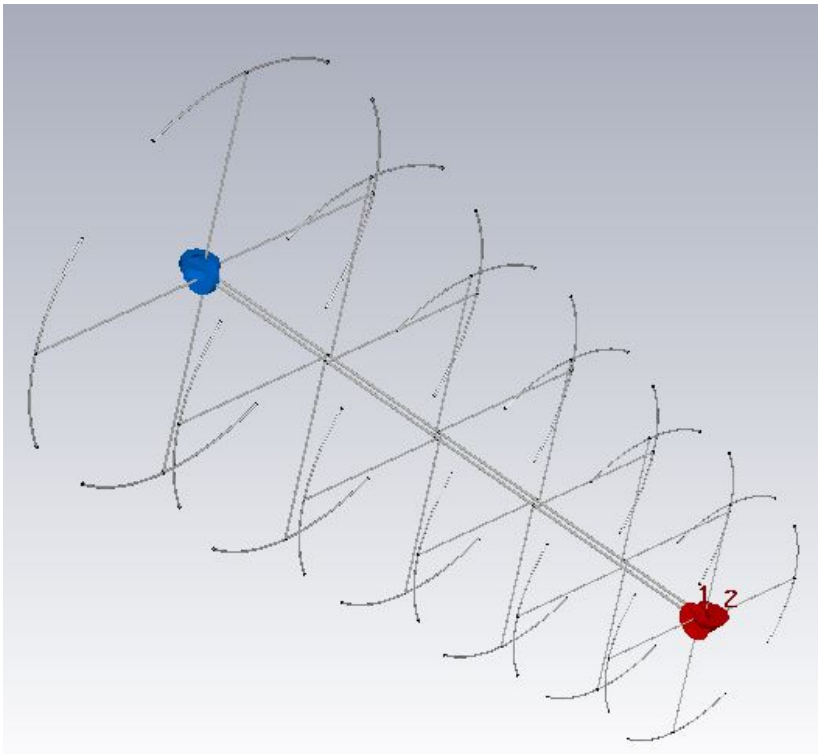

Figure 3.17. Compact CP LPDA 6-element design.

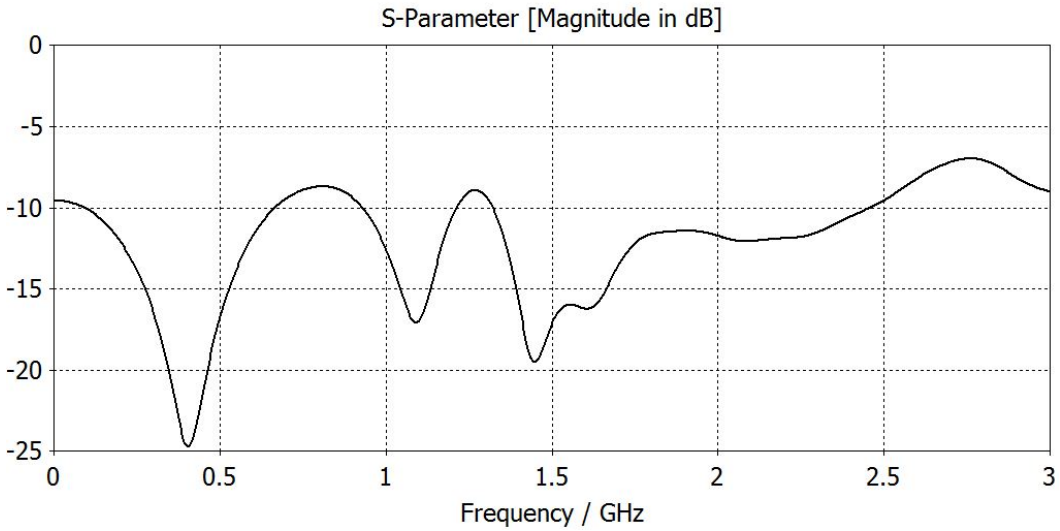

Figure 3.18. Full-size CP LPDA 6-element frequency vs. S_{11}.

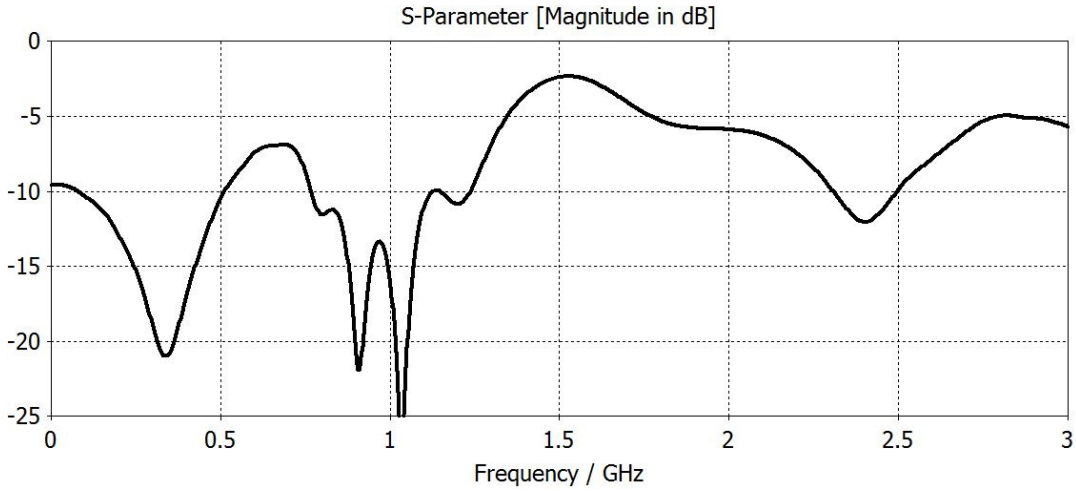

Figure 3.19. Compact CP LPDA 6-element frequency vs. S_{11}.

Next, the farfield properties of the antenna designs are analyzed. The realized gain curves are shown in Figures 3.20 and 3.21. In the full-size 6-element design, a high realized gain value is achieved throughout most of the frequency band, with a peak of

8.12 dBic at 1.6 GHz. As expected, the realized gain is low in the compact 6-element design due to impedance mismatch. The realized gain plummets to -23 dBic at 2 GHz.

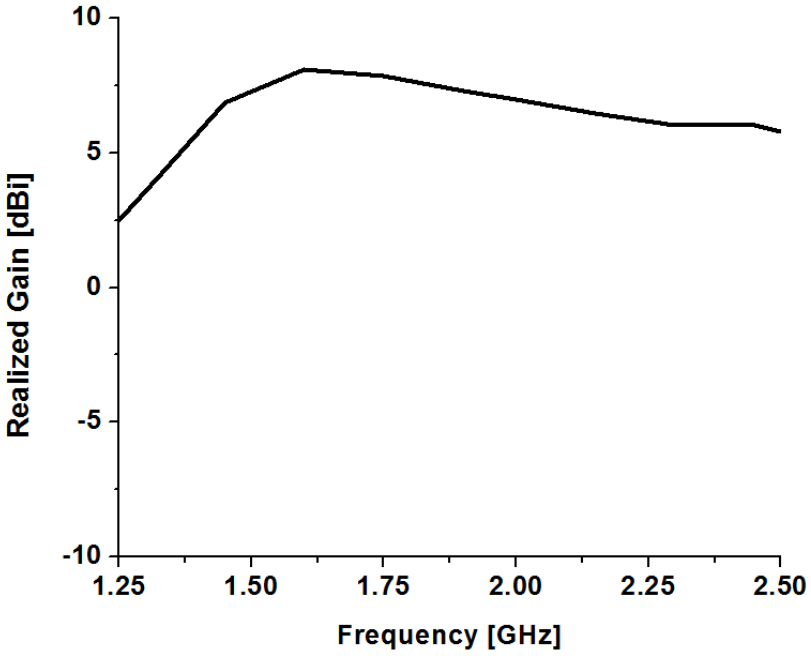

Figure 3.20. Full-size CP LPDA 6-element frequency vs. realized gain.

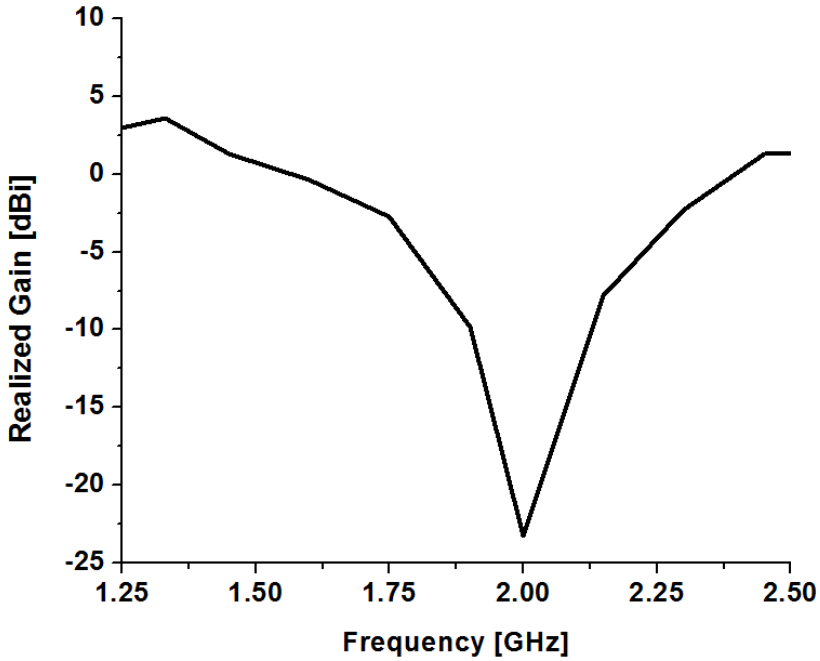

Figure 3.21. Compact CP LPDA 6-element frequency vs. realized gain.

The axial ratio of the full-size and compact 6-element designs can be seen in Figures 3.22 and 3.23, respectively. The full-size design is seen to be circularly polarized across the frequency band of interest, while the compact design is only circularly polarized for roughly half of the frequency band. From the data in the S_{11} curves and farfield properties of both antennas, the T-top loading is seen to be ineffective in this case. However, the alternate approach to use a uniform wire radius on the CP LPDA with 11-elements is still viable for antenna fabrication, despite being more elements. The unification of wire radius on the elements will make the fabrication process feasible.

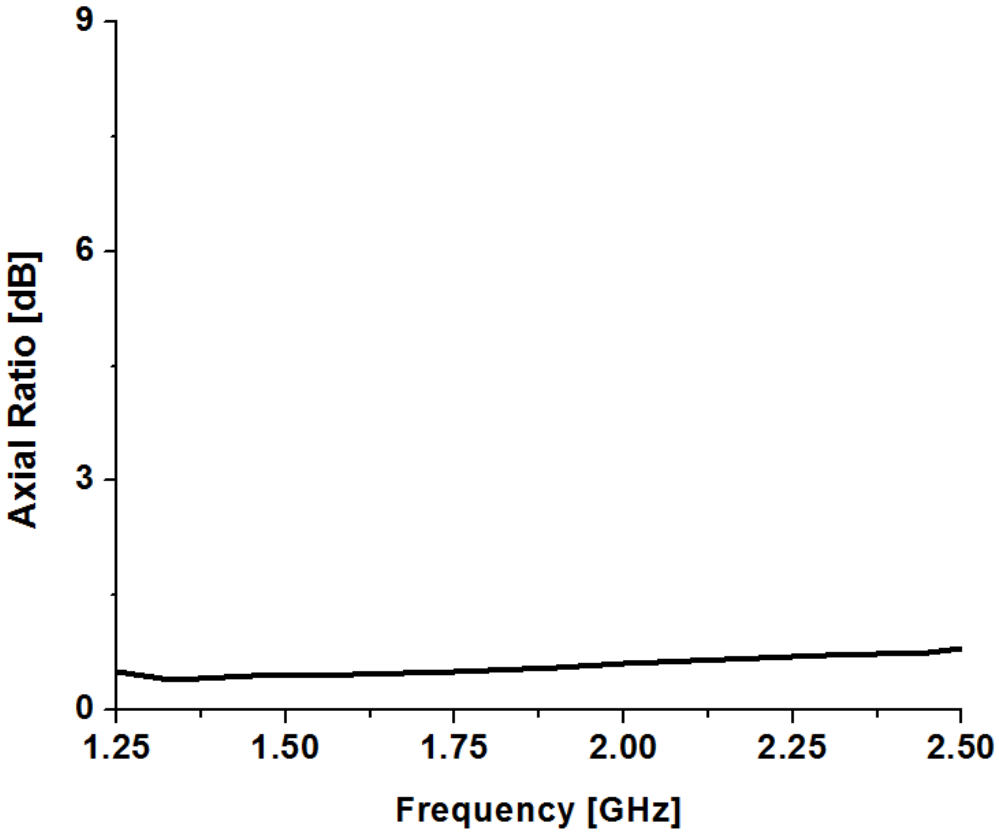

Figure 3.22. Full-size CP LPDA 6-element frequency vs. axial ratio.

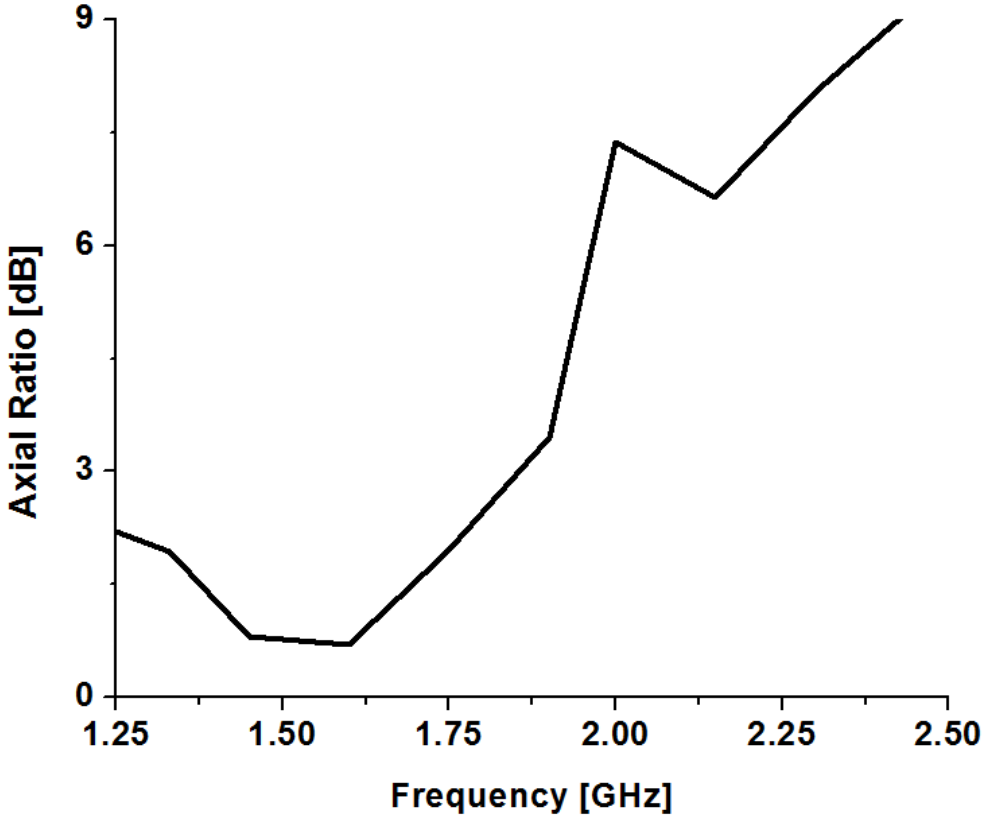

Figure 3.23. Compact CP LPDA 6-element frequency vs. axial ratio.

3.4.2 Uniform Wire Radius

The alternate approach to prepare the compact CP LPDA for fabrication is to use a single wire radius for the entire antenna design. The wire radius must be small enough to accompany the small spacing between the four transmission lines. If the wire radius is too big, the transmission lines touch and the antenna doesn't work. So, a wire radius of 0.2 mm is chosen (AWG # 26). The frequency vs. S_{11} curves in Figure 3.24 and 3.25 of the full-sized and compact uniform wire radius designs show the resulting impedance bandwidths. The full-size design shows a nearly identical S_{11} to that of the non-uniform wire radius design. The -10 dB bandwidth covers from 0.77 GHz to 2.42 GHz.

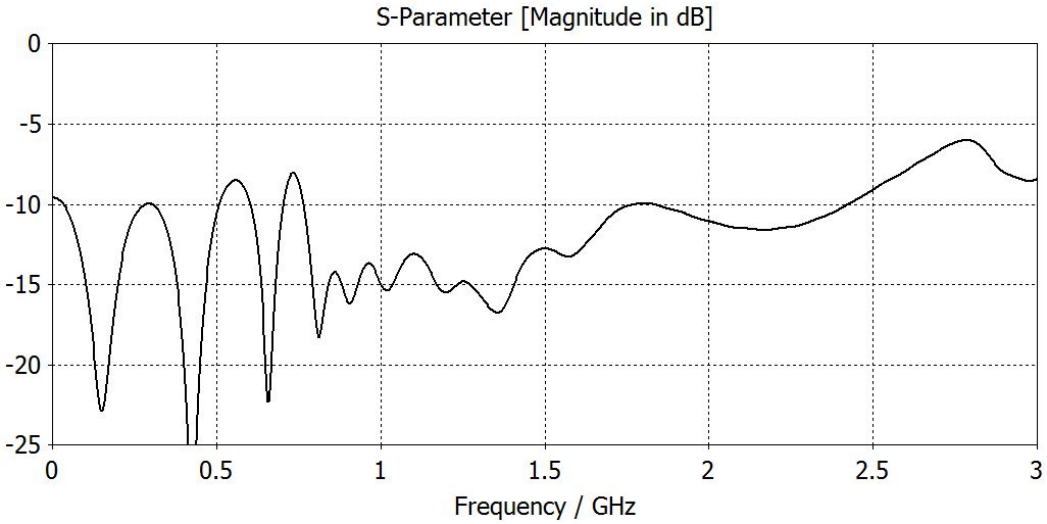

Figure 3.24. Full-size CP LPDA with uniform wire radius frequency vs. S_{11}.

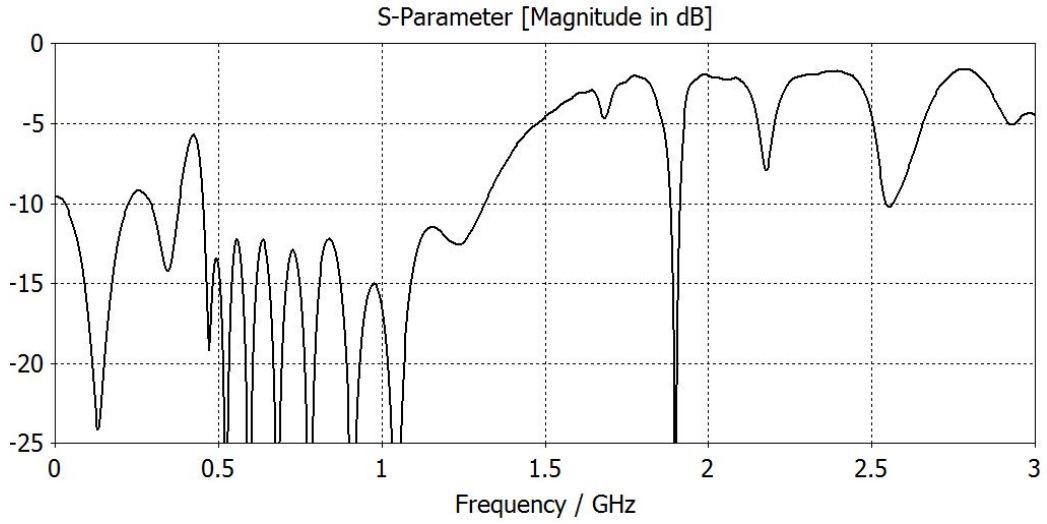

Figure 3.25. Compact CP LPDA with uniform wire radius frequency vs. S_{11}.

The S_{11} of the compact CP LPDA with uniform wire radius results in poor performance. With poor impedance matching, a low realized gain is inevitable. The frequency vs. realized gain curve of the full-sized CP LPDA is shown in Figure 3.26, and its frequency vs. axial ratio curve is shown in Figure 3.27. For the compact CP LPDA

with uniform wire radius, the axial ratio is very likely to follow the previous trend of the compact 6-element CP LPDA design where the antenna is not circularly polarized across the entire operating frequency band. Thus, the results are not presented.

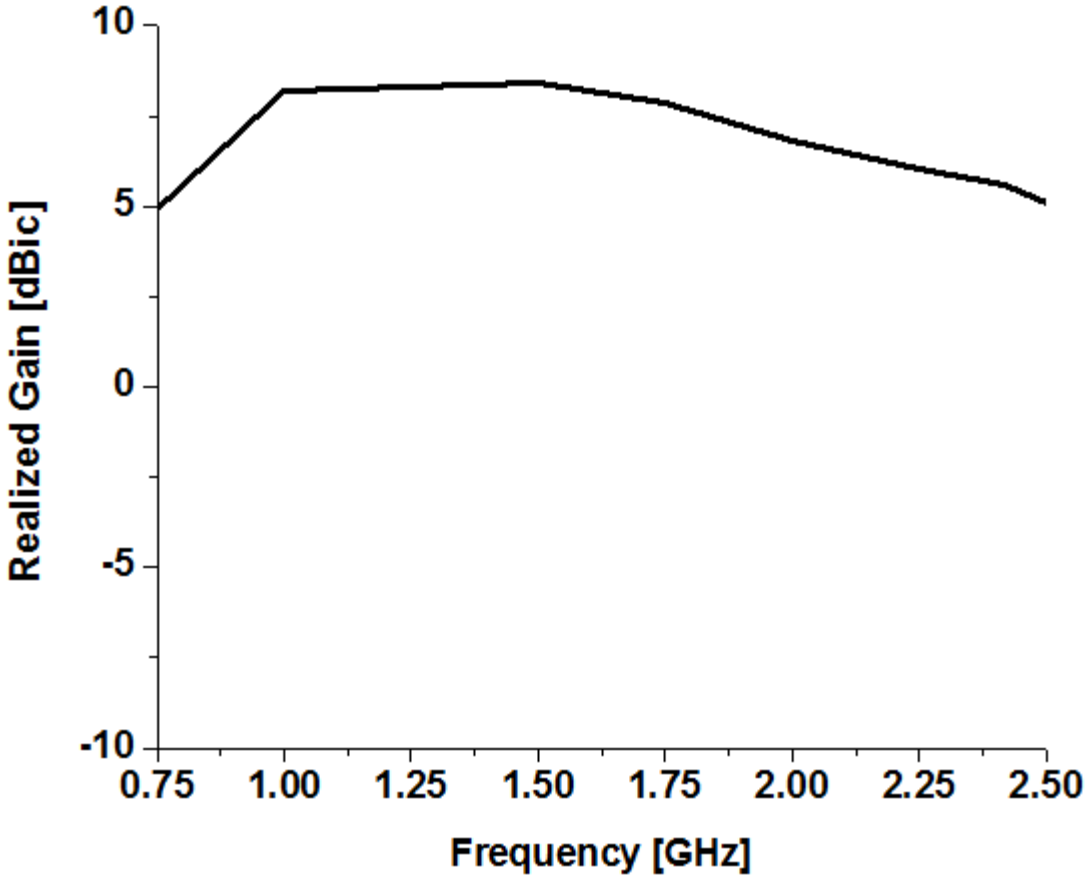

Figure 3.26. Full-size CP LPDA uniform wire radius frequency vs. realized gain.

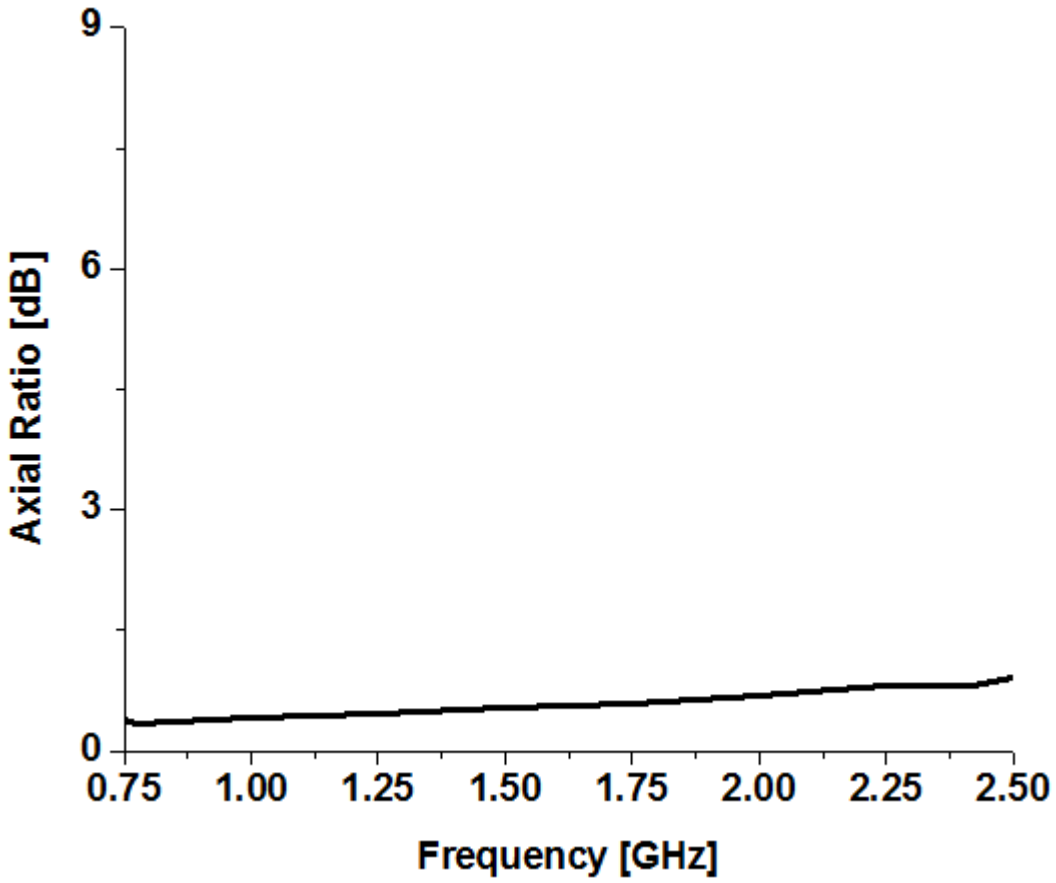

Figure 3.27. Full-size CP LPDA uniform wire radius frequency vs. axial ratio.

3.5 Summary

From the results of both the reduction in number of elements and using a uniform wire radius, the compact design with top-loading in either of these cases is not feasible. However, this could possibly be due to the fact that the original antenna design is being modified before top-loading. If a new full-size CP LPDA were to be generated through Antenna Magus that were 6-elements, it could possibly be modified to have a uniform wire radius, T-top loaded, and produce good results.

CHAPTER 4

CONCLUSION

4.1 Conclusion of Presented Work

Two novel antenna designs are presented and analyzed. Both antennas are circularly polarized and utilize T-top loading for miniaturization. The circularly polarized planar cross dipole is electrically small with a *kr* of 0.65. While the entire compact CP LPDA is not electrically small, it consists of 0.8 *kr* dipole elements that are electrically small, effectively reducing the overall volume of the antenna.

Chapter 2 presents an electrically small, CP planar cross dipole antenna. CP is generated using a crossed dipole structure consisting of unequal length dipoles. Top loading is employed on the end of each dipole to achieve an electrical size, *kr*, of 0.65. Short stubs are used to boost the low radiation resistance encountered due to the electrically small size of the antenna. A maximum RG of 1.37 dBic was obtained.

In chapter 3, a new method of reducing the size of a λ/2 element LPDA is presented, on which the T-top CP LPDA design is based. The design employs top-loading onto two orthogonal linear LPDAs with a 90° phase difference between feeds. Simulation results look promising, but modification of the design for fabrication and measurements is necessary. In an attempt to facilitate fabrication, simulations involving a reduction in the number of elements and using a uniform wire radius are performed. The full-size designs of these simulations prove effective, but the top-loading onto these designs results in poor impedance matching.

6.2 Future Work

In chapter 2, the circularly polarized planar cross dipole is presented with an electrical size, *kr*, of 0.65. Further miniaturization is possible by either increasing top-loading lengths, as seen in Figure 4.1, or by utilizing both the front and back of the substrate for increasing top-loading lengths or creating a parasitic element design.

In chapter 3, the 11-element non-uniform wire radius compact CP LPDA design is presented with promising results. However, no good results have been achieved yet with a design that is easier to fabricate. Future work in redesigning the full-size CP LPDA in Antenna Magus and then top-loading that design could provide good results. Also, employing the T-top loading structure on a single-feed CP LPDA could prove a much better antenna design by eliminating the need for a phase shift on the feed and by using only a single feed rather than two. To accomplish this design, an optimization with many variables would need to be performed with varying top-loading lengths rather than a fixed one, such as the design in Figure 4.2.

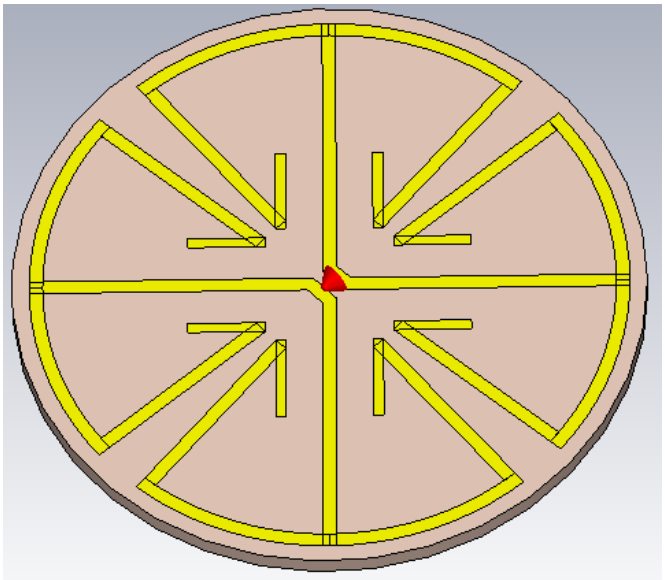

Figure 4.1. Planar cross dipole with further miniaturization (*kr* = 0.5).

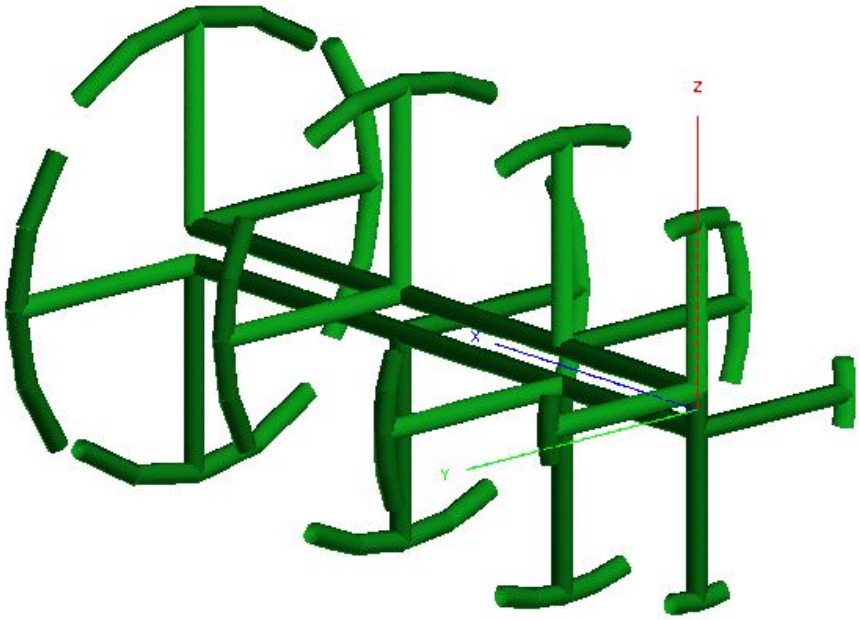

Figure 4.2. Compact CP LPDA with single feed.

REFERENCES

Anagnostoul, D. E., J. Papapolymerou, M. M. Tentzeris, and C. G. Christodoulou. "A Printed Log-Periodic Koch-Dipole Array (LPKDA)." *IEEE Antennas and Propagation Letters*, 2008: 456-460.

Bai, J., S. Shi, J. P. Wilson, R. Nelson, and D. W. Prather. "Wideband, electrically small, planar, coupled subwavelength resonator antenna with an embedded matching network." *IEEE Transactions on Antennas and Propagation*, 2013: 2388-2396.

Balanis, C. A. *Antenna Theory Analysis and Design.* Hoboken: John Wiley & Sons, 2005.

Bolster, M. F. "A New Type of Circular Polarizer Using Crossed Dipoles." *IRE Transactions on Microwave Theory and Techniques*, 1961: 385-388.

Chu, L. J. "Physical Limitation of Omni-Directional Antennas." *Journal of Applied Physics*, 1948: 1163-1175.

Isbell, D. "Log periodic dipole arrays." *IRE Transactions on Antennas and Propagation*, 1960: 260-267.

Jardon-Aguilar, H., J.A. Tirado-Mendez, R. Flores-Leal, and R. Linares-Miaranda. "Reduced Log-periodic Dipole Antenna Using Cylyindrical-Hat Cover." *IET Microwaves, Antennas and Propagation*, 2010: 1697-1702.

Kuo, S. "Size-reduced log-periodic dipole array." *IEEE Antennas Propagation Society International Symposium.* 2008. 456-460.

Lim, S., R. L. Rogers, and H. Ling. "A tunable electrically small antenna for ground wave transmission." *IEEE Transaction on Antennas and Propagation*, 2006: 417-421.

Nalbandian, V., and C. S. Lee. "Planar, single-feed, circularly polarized microstrip antenna with enhanced bandwidth." *IEEE Antennas Propagation Society International Symposium.* 1998. 1368-1371.

Rhodes, D. S., and S. Lim. "Size reduction of the Log-Periodic Dipole Array." *Antennas and Propagation Society International Symposium.* 2013. 1578-1579.

Sievenpiper, D. F., et al. "Experimental Validation of Performance Limits and Guidelines for Small Antennas." *IEEE Transactions on Antennas and Propagation*, 2012: 8-19.

Stutzman, W. L. *Antenna Theory and Design.* New Jersey: John Wiley & Sons, 1998.

Suwalak, R., and C. Phongcharoenpanich. "Circularly polarized truncated planar antenna with single feed for UHF RFID reader." *Proceedings of Asia-Pacific Conference on Communications.* 2007. 103-106.

Wheeler, H. A. "Fundamental limitations of small antennas." *Proceedings of the IRE.* 1947. 1479-1484.

Yu, J., and S. Lim. "Design of an electrically small, circularly polarized, parasitic array antenna for an active 433.92-MHz RFID handheld reader." *IEEE Transactions on Antennas and Propagation*, 2012: 2549-2554.